The Integrated Terminal Weather System Terminal Winds Product

Rodney E. Cole and F. Wesley Wilson

The wind in the airspace around an airport impacts both airport safety and operational efficiency. Knowledge of the wind helps controllers and automation systems merge streams of traffic; it is also important for the prediction of storm growth and decay, burn-off of fog and lifting of low ceilings, and wake vortex hazards. This knowledge is provided by the Integrated Terminal Weather System (ITWS) gridded wind product, or Terminal Winds. The Terminal Winds product combines data from a national numerical weather-prediction model, called the Rapid Update Cycle, with observations from ground stations, aircraft reports, and Doppler weather radars to provide estimates of the horizontal wind field in the terminal area. The Terminal Winds analysis differs from previous real-time winds-analysis systems in that it is dominated by Doppler weather-radar data. Terminal Winds uses an analysis called cascade of scales and a new winds-analysis technique based on least squares to take full advantage of the information contained in the diverse data set available in an ITWS. The weather radars provide sufficiently fine-scale winds information to support a 2-km horizontal-resolution analysis and a five-minute update rate.

A prototype of the Terminal Winds analysis system was tested at Orlando International Airport in 1992, 1993, and 1995, and at Memphis International Airport in 1994. The field operations featured the first real-time winds analysis combining data from the Federal Aviation Administration TDWR radar and the National Weather Service NEXRAD radar. The evaluation plan is designed to capture both the overall system performance and the performance during convective weather, when the fine-scale analysis is expected to show its greatest benefit.

Atmospheric conditions in the terminal area have a significant impact on airport operations and safety. A number of Federal Aviation Administration (FAA) systems under development to improve airport safety and capacity require knowledge of the wind and other atmospheric variables. These systems include (1) the Center TRACON Advisory System (CTAS) to automate air traffic control to optimize fuel consumption, scheduling, and aircraft merging and separations [1]; (2) the Wake Vortex Advisory System (WVAS) to reduce aircraft separations for wake vortex avoidance; (3) the Integrated Terminal Weather System (ITWS) windshift and runway-winds prediction systems to predict wind shifts—from gust fronts and other sources—that lead to runway reconfiguration; (4) the ITWS low ceiling and visibility predictions [2]; and (5) the ITWS convective storm growth-and-decay predictions. Figure 1 illustrates the different aviation systems, and shows where in the terminal airspace each system has the most impact and utility.

Currently in development by the FAA, ITWS will produce a fully automated, integrated terminal weather information system to improve the safety, efficiency, and capacity of terminal-area aviation operations [3]. This system will acquire data from FAA and

National Weather Service radar sensors as well as from aircraft in flight in the terminal area, and it will provide air traffic control personnel with weather information products that are immediately usable without further meteorological interpretation. These products include current terminal-area weather and short term (zero to thirty minute) predictions of significant weather phenomena.

The ITWS gridded analysis system will provide current-time estimates and short-term forecasts of wind, temperature, moisture, and atmospheric pressure at each point in a three-dimensional grid in the terminal area. Estimates of these quantities are currently produced by national-scale forecast models at the National Weather Service, although these national-scale models are on coarse grids in space and time, relative to airport operations. To support the special requirements of aviation systems, the ITWS gridded analysis system will improve the resolution and timeliness of the estimates from the national-scale models by incorporating additional information from terminal-area sensors.

We have concentrated our initial development efforts on gridded horizontal winds, with a gridded temperature analysis to follow. There are three reasons for choosing this sequence of development: (1) horizontal winds and wind changes have a direct impact on aviation operations and in the automated aviation systems mentioned above; (2) high-resolution horizontal wind data are provided by meteorological Doppler radars (each ITWS is expected to have data from at least one Doppler radar, and often two or more, which makes winds analysis tractable in the near term); and (3) horizontal winds are an important factor in many meteorological processes because they contribute to the transport of momentum, heat, and

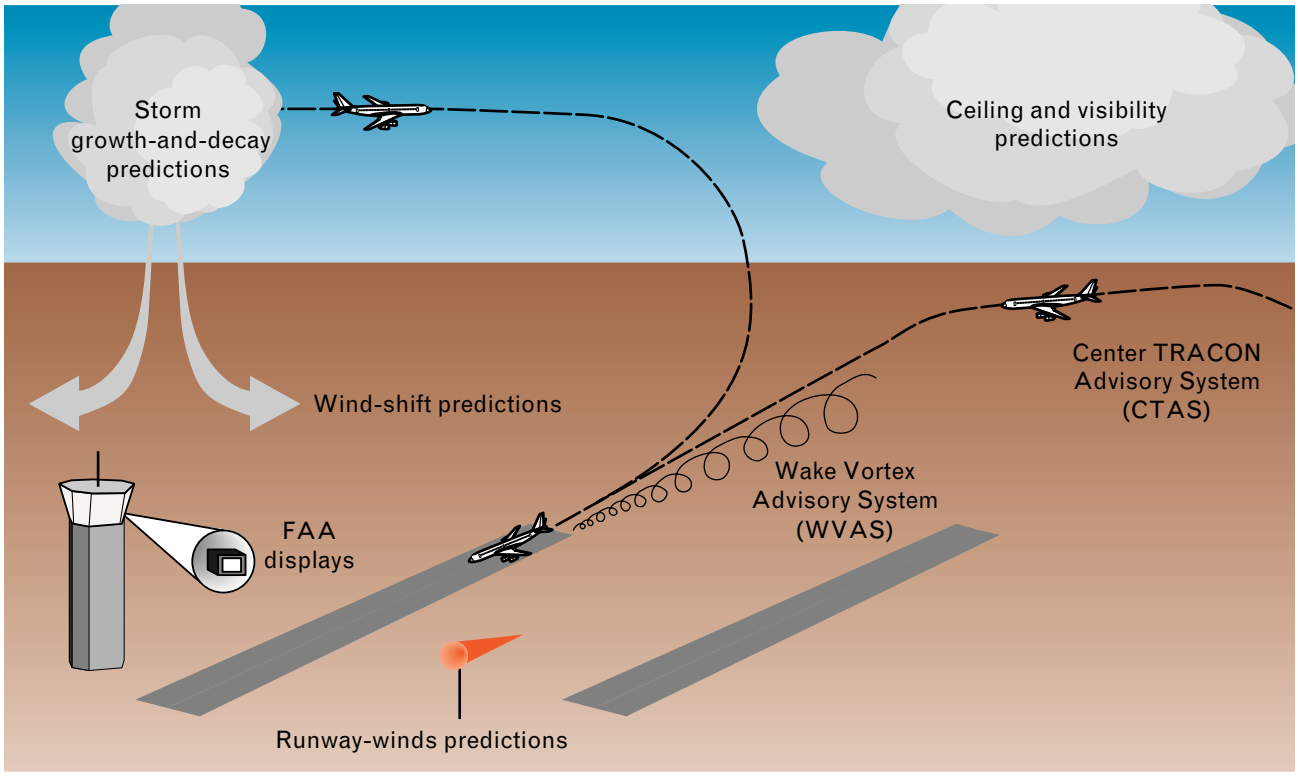

FIGURE 1. Aviation systems supported by the ITWS gridded horizontal winds product, or Terminal Winds. Systems requiring Terminal Winds information are being developed to automate air traffic control to optimize fuel consumption, scheduling, and aircraft separation (the Center TRACON Advisory System, or CTAS); reduce aircraft separation for wake vortex avoidance (the Wake Vortex Advisory System, or WVAS); predict wind shifts from gust fronts and other sources that would lead to runway reconfiguration (the ITWS wind-shift and runway-winds prediction systems); predict the onset and dissipation of fog and low-ceiling conditions; and predict storm growth and decay.

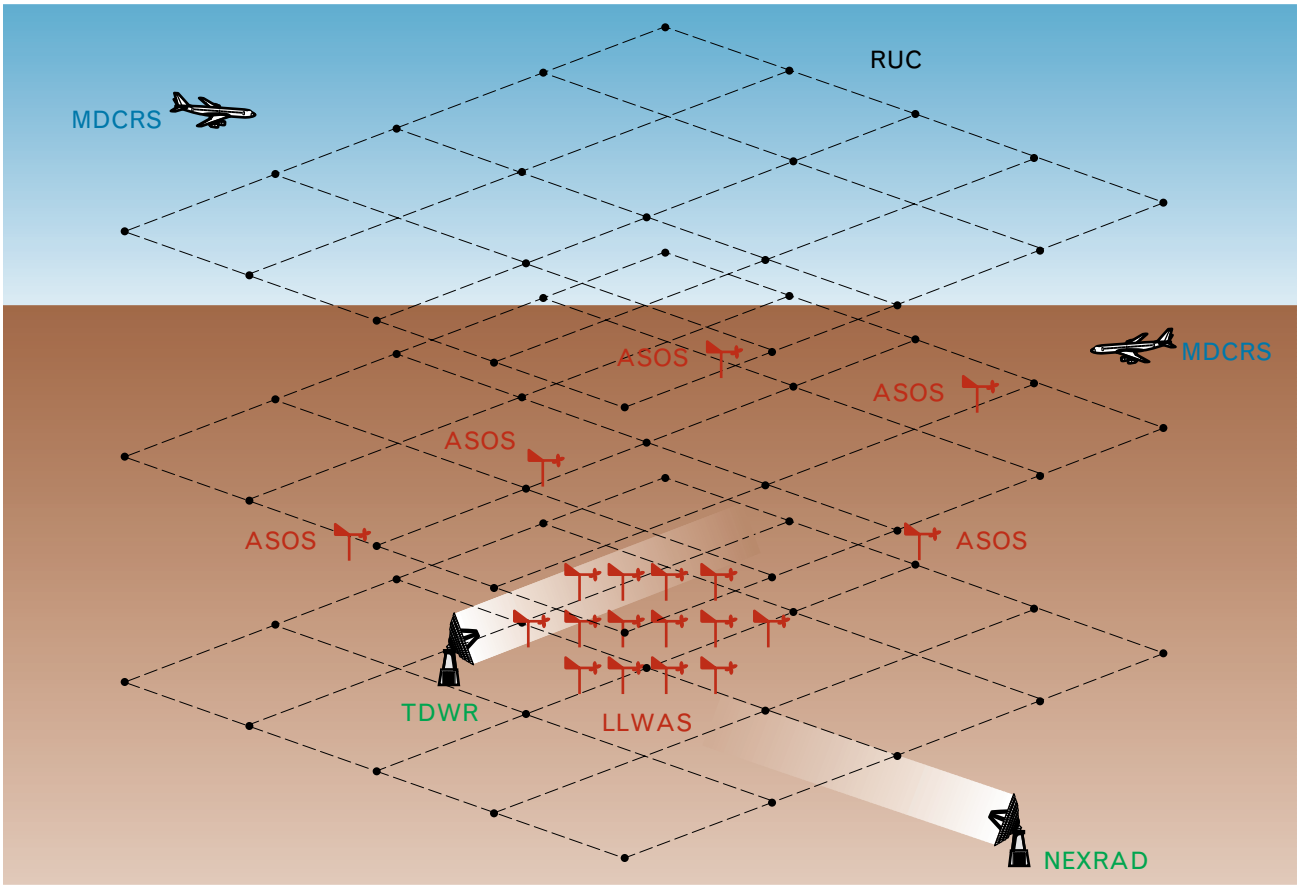

FIGURE 2. Data sources for Terminal Winds. These sources are a national-scale forecast model called Rapid Update Cycle (RUC) provided by the National Weather Service; meteorological Doppler radars including the Terminal Doppler Weather Radar (TDWR) and the National Weather Service WSR-88D (NEXRAD) radar; commercial aircraft using the Meteorological Data Collection and Reporting System (MDCRS); and Automated Surface Observing System (ASOS) and Low Level Wind Shear Alert System (LLWAS) surface anemometers.

humidity (in particular, the gridded temperature analysis and the gridded humidity analysis depend on the gridded winds analysis).

The ITWS gridded horizontal winds product, or Terminal Winds, was developed to provide detailed knowledge of the winds in the terminal airspace to each of the aviation systems illustrated in Figure 1. Terminal Winds obtains wind information from a number of sources, including a national-scale forecast model called Rapid Update Cycle (RUC) provided by the National Weather Service; meteorological Doppler radars, including the FAA's Terminal Doppler Weather Radar (TDWR) and the National Weather Service WSR-88D (NEXRAD) radar; commercial aircraft using the Meteorological Data Collection and Reporting System (MDCRS); and the Automated Surface Observing System (ASOS) and Low Level Wind Shear Alert System (LLWAS) surface anemometers. The design of the Terminal Winds analysis system must take into account the weather phenomena to be captured, sensor characteristics, and nonuniform and dynamic data distributions; the system must also be robust to sensor failures. Figure 2 illustrates the location and variety of the data sources used in the Terminal Winds analysis.

In the summer of 1992 an initial Terminal Winds prototype [4, 5] based on the Local Analysis and Prediction System (LAPS) developed at the National Oceanic and Atmospheric Administration's (NOAA) Forecast Systems Laboratory (FSL) [6, 7] was tested in the Lincoln Laboratory ITWS testbed in Orlando, Florida. This prototype featured the first real-time

winds analysis using data from the TDWR radar [8] and the NEXRAD radar [9].

Based on lessons learned from the 1992 test, a new analysis technique was developed to extract the wind information in the Doppler radar data more effectively. This new technique, called *optimal estimation*, uses a minimum-error-variance technique (least squares) and is closely related to both the state-of-the-art operational non-Doppler winds-analysis technique, called *optimal interpolation*, and standard multiple-Doppler techniques. The optimal-estimation technique was evaluated on the 1992 Orlando data set, and demonstrated in real time in the Orlando testbed during the summer of 1993, in Memphis during the spring and summer of 1994, and in Orlando during the winter of 1995. The optimal-estimation-based analysis provides a significant improvement over previous winds analyses using Doppler radar data.

In the next section we discuss design considerations that motivated the development of the Terminal Winds system. Then we give an overview of the Terminal Winds system, and provide a description of the analysis with particular attention to Doppler data analysis and the optimal-estimation analysis. Finally, we give an overview of our product accuracy evaluation based on data collected in the Orlando testbed, and we discuss the direction of future work. The section entitled "Details of the Terminal Winds Analysis" can be omitted by readers interested only in an overview of the Terminal Winds system.

Design Considerations

There are a number of design considerations for a winds-analysis system that will support the aviation systems listed above and operate with information from sensors in the terminal area. Ideally, users of the gridded winds analyses levy performance requirements for resolution, accuracy, and timeliness. The automated aviation systems that rely on these analyses, however, are still under development, and final performance requirements are not yet completely determined. We have taken the approach of basing resolution, accuracy, and timeliness on expected wind-field phenomenology and sensor characteristics, with the goal of minimizing the norm of the wind-vector error in the analyzed wind fields.

There are a variety of information sources available for the gridded winds analysis, including forecast models, surface observing systems, commercial aircraft, and meteorological Doppler radars. These data sources provide information of differing content, accuracy, and resolution. The gridded winds analysis system must correctly resolve important wind-field features by assembling this diverse information, and must be robust when sensors unexpectedly go off line or come back on line.

Wind-Field Phenomenology

The terminal airspace extends from the airport surface to 18,000 feet mean sea level (MSL). Meteorologically, this airspace is divided into two regimes. The portion of the atmosphere closest to the Earth's surface is referred to as the *planetary boundary layer* (PBL), and its dynamical structure is strongly influenced by surface effects. The atmosphere in the PBL is well mixed during daylight hours, and solar heating of the Earth's surface often expands the PBL to as much as 6000 feet above ground level. At night, when the air is relatively cool (and less well mixed), the PBL may extend to less than 300 feet above ground level. A mixture of wind-field features can coexist in the PBL with a wide range of spatial and temporal scales. Features with spatial scales smaller than a few kilometers or temporal scales shorter than a few minutes, however, are not important to the users of the gridded winds analysis. These small-scale features do not, for example, affect time of flight.

The region above the PBL is referred to as the *free atmosphere* because of its relative insulation from surface effects. The free atmosphere is usually composed of large-scale wind features, each with horizontal extent of at least tens of kilometers and lasting tens of minutes. Small-scale wind features can exist in the free atmosphere—for example, within thunderstorms—but are rare.

Information Sources

The underpinning of the Terminal Winds system is provided by the RUC, which is a numerical weather-prediction model run by the National Meteorological Center of the National Weather Service. The RUC is based on the Mesoscale Analysis and Prediction Sys-

tem (MAPS) developed at NOAA's FSL [10]. Horizontal wind measurements are provided at the surface near an airport by LLWAS anemometers [11] and in outlying regions by ASOS anemometers [12]. MDCRS-equipped aircraft provide measurements of the horizontal winds aloft [13]. These aircraft are not widely distributed but are typically located along routes of commercial air traffic, making them an important source of information about winds in the free atmosphere.

The ITWS will also have information from the two meteorological Doppler radars mentioned above—the TDWR and the NEXRAD radar. Doppler radars provide measurements of a single component of the wind, the radial component directed toward the radar. These radars provide the vast majority of the information coming into the Terminal Winds system, although the other data sources also play an important role, especially in the free atmosphere.

Table 1 shows that the information from the different data sources differs widely in spatial and temporal resolution, as well as in content and accuracy. The accuracy listed is relative to an average wind over a disk with a 3-km radius in the horizontal during a time span on the order of a few minutes. For example, Doppler radars provide accurate information on winds at specific points in space, but these values can reflect small-scale features that are considered noise in the Terminal Winds system, which reduces their effective accuracy. Because of the 60-km grid spacing, RUC cannot resolve most thunderstorm-scale weather phenomena (there are plans to reduce the horizontal resolution to 10 km and the update rate to one hour by the end of the decade). MDCRS-equipped aircraft measurements are available only at random positions and times along flight paths of commercial aircraft, with a data latency of at least fifteen minutes. On average, approximately ten MDCRS reports are received per hour. Surface stations such as LLWAS and ASOS anemometers vary in update rate between ten seconds and twenty minutes, and Doppler radars provide only a single component of the wind. Combining these widely varying sources of information is a significant technical challenge.

Meteorological Doppler radars provide estimates of the wind-velocity component along the radar beam (radial velocities) as well as measurements of return intensity (reflectivity). These radars cannot directly measure the wind-velocity component perpendicular to the radar beam. The radial-velocity wind estimates are derived from the phase shift in returns from airborne reflectors such as bugs, water droplets, and refractive index inhomogeneities that are assumed to be traveling with the wind. Doppler radars provide accurate and dense measurements only in regions with sufficient reflectors.

Doppler radars provide high-resolution radial-velocity wind information throughout the PBL because atmospheric mixing tends to distribute the particles that serve as reflectors for the Doppler radars. This phenomenon allows the gridded analysis to provide high-resolution wind information in the PBL, where small-scale wind structures are expected. Because of fewer reflectors in the free atmosphere above the PBL,

Table 1. Characteristics of Data Sources for Terminal Winds

Source	*Update Rate (min)*	*Horizontal Resolution*	*Accuracy (m|sec)*	*Information Content*
RUC	180	60 km	2–7	vector
TDWR	5	0.120 km x 0.5°	1–2	single component
NEXRAD	6	0.250 km x 1°	2–4	single component
MDCRS	variable	variable	4	vector
ASOS	20	≈60 km	2	vector
LLWAS	0.16 (10 sec)	2–3 km	1	vector

Doppler information is often available but sparse. The RUC and MDCRS information sources play an important role at these altitudes. The lower-resolution information available aloft from these two sources, as well as from Doppler radars, is usually appropriate for the expected scales of the wind-field dynamics above the PBL. In regions of convective activity where small-scale wind structures are likely to exist above the PBL, the Doppler radars continue to provide substantial amounts of information.

In regions with information from two or more Doppler radars, a linear system of equations can be solved to estimate the horizontal winds [14]. The details of this multiple-Doppler analysis are given in the next section. The quality of the estimate derived from this linear system of equations varies depending on the range of radar azimuth angles associated with the Doppler data and the separations between the locations of the data in space and time. If Doppler data are available for two independent directions at the same location and time, the resulting estimate will be of high quality. If the Doppler data are all from nearly the same direction or are widely separated, the resulting estimate will be of lower quality.

Overview of the Terminal Winds Analysis

The Terminal Winds analysis is based on the following design goals related to the above considerations. The analysis should (1) respect the variety of spatial and temporal scales of wind-field features in the PBL and above the PBL, (2) respect the variety of spatial and temporal scales of the information from the different data sources, (3) respect the differing quality of information from the different sources, (4) properly merge vector information with single-component information, (5) properly interpolate nonuniformly distributed information, (6) provide a smooth transition from regions of dense data to regions of sparse data, (7) take advantage of the information content of a multiple-Doppler data set while respecting the varying quality of that information, (8) handle fluctuations in data availability, and (9) minimize the magnitude of the error in the wind-vector estimates.

The primary philosophy of the Terminal Winds analysis is that the national-scale forecast model provides an overall picture of the winds in the terminal airspace, although painted in broad strokes. Information from the terminal sensors is then used to fill in detail and correct the broad-scale picture. Of course, the corrections and added detail can be provided only in those regions with nearby data. What constitutes "nearby" depends on the spatial and temporal scale of the feature to be captured in the analysis. The refinement of the broad-scale wind field is accomplished by averaging the model forecasts with current data. This averaging allows the analysis technique to produce wind vectors that vary smoothly from regions with a large number of observations to regions with few observations or no observations at all, and enables the analysis to cope gracefully with unexpected changes to the suite of available sensors.

To account for the different scales of wind features and the differing resolution of the information provided from the various sensors, the Terminal Winds analysis employs a *cascade-of-scales* analysis. This cascade-of-scales analysis uses nested grids, with an analysis using a 2-km horizontal resolution and a 5-min update rate nested within an analysis using a 10-km horizontal resolution and 30-min update rate, which in turn is nested within the RUC forecast using a 60-km horizontal resolution and 180-min update rate. All the data sources are used in the 10-km-resolution analysis, and data are allowed to be as old as ninety minutes. Only the information from the Doppler radars and the LLWAS anemometers, however, are suitable for the 2-km-resolution analysis. The cascade-of-scales analysis is appropriate for the different scales of wind-field features that need to be captured in the analysis, as well as the different scales of information provided by the different data sources, and the cascade-of-scales analysis provides a uniform level of refinement at each step of the cascade. An additional benefit is that the 10-km-resolution analysis acts as a stand-in for the planned 10-km-resolution national forecast. When a 10-km national forecast becomes available, the 10-km ITWS analysis can be dropped.

An important goal is the minimization of the error of the analyzed wind field. To achieve this goal the Terminal Winds analysis uses a least-squares technique, which is designed to average vector quantities and single-component quantities jointly. Previous state-of-the-art operational winds-analysis systems

have used statistical techniques to great advantage. None of these systems, however, have the ability to analyze the data from Doppler radars directly. The Terminal Winds analysis represents a substantial step forward in winds analysis, which is especially important because increasing numbers of Doppler weather radars are being deployed.

The least-squares technique used in the Terminal Winds analysis accounts for the variations in quality of the information available to the Terminal Winds analysis, as well as errors arising from data age and errors arising from estimating winds at locations removed from the observation location. The least-squares technique also corrects for correlated errors. Highly correlated errors arise frequently because of the nonuniform distribution of data from the Doppler radars. Often the Terminal Winds analysis estimates the wind at locations with many Doppler values clumped together at a distance, and few data values elsewhere. Because of the nonhomogeneity of the wind field, the data values in the region of Doppler information contain highly correlated errors, relative to the wind at the distant analysis point. If this error correlation is not accounted for, these data values dominate the analysis to a greater degree than warranted by their information content. This situation is illustrated by an example later.

Details of the Terminal Winds Analysis

The details of the cascade-of-scales analysis and statistical analysis are given in this section. The reader may skip to the next section without losing the continuity of the exposition.

The Terminal Winds analysis system is designed to achieve the nine goals stated in the previous section. The next subsection describes the method used to achieve the goal of respecting the variety of spatial and temporal scales both within the PBL and in the free atmosphere above the PBL, as well as the goal of properly merging information from data sources with differing spatial and temporal update rates. The following subsections provide general background information on winds analysis from meteorological Doppler radar data. These subsections discuss the types of errors found in Doppler data, the method used to produce regionally representative wind estimates on a Cartesian grid from point measurements in spherical coordinates, and the traditional method for estimating horizontal winds from multiple-Doppler data sets. The last topic is especially germane to the development of the optimal-estimation technique. Finally, we present a subsection on the optimal-estimation technique, and conclude this section of the article with a subsection on illustrative examples.

Cascade-of-Scales Analysis

Within the PBL or inside regions of convective weather, the Terminal Winds analysis needs to be able to resolve wind-field structures that have spatial scales as small as a few kilometers, and that evolve on time scales as small as several minutes. Above the PBL and outside regions of convective weather, the analysis needs to be able to resolve wind-field structures with spatial scales and temporal scales that are about an order of magnitude larger. To capture the differing scales of wind structures while respecting the differences in information content of the various sources, Terminal Winds uses a cascade-of-scales analysis.

The cascade-of-scales analysis starts with an RUC forecast having a 60-km horizontal-resolution grid and a 3-hr update rate. The RUC data are used to initialize an analysis with a 10-km horizontal-resolution grid and a 30-min update rate. The 10-km-resolution wind field is used in turn to initialize an analysis with a 2-km horizontal-resolution grid and a 5-min update rate. Each analysis grid has a vertical resolution of 50 millibars of atmospheric pressure; Table 2 gives the nominal altitudes for the analysis levels in both millibars and feet. All of the data sources are used in the 10-km-resolution analysis, but only Doppler data and LLWAS data are used in the 2-km-resolution analysis. The cascade-of-scales analysis matches the atmospheric dynamics and information content of the different data sources, and gives a uniform ratio of refinement as the analysis steps from coarser to finer resolution. Stepping down this cascade of scales, the ratios for temporal resolution are both 6:1, and the ratios for horizontal resolution are 6:1 and 5:1, as shown in Table 3. The nested cascade-of-scales analysis grids simplify the software implementation.

Ideally, the cascade-of-scales analysis would provide a refinement of the vertical resolution from one

Table 2. Pressure Levels in Millibars in the Cascade-of-Scales Analysis, and Corresponding Altitudes in Feet (MSL)

Altitude in millibars	*Altitude in feet*
1000	360
950	1770
900	3240
850	4780
800	6390
750	8090
700	9880
650	11,780
600	13,800
550	15,960
500	18,290
450	20,810
400	23,580
350	26,633
300	30,070
250	34,000
200	38,770
150	44,760
100	53,190

analysis scale to the next. A Doppler radar provides high-horizontal-resolution wind measurements, but does not provide high vertical resolution except near the radar. The current Terminal Winds system uses the same 50-mb vertical resolution for the 10-km analysis as for the 2-km analysis. In the future we plan to examine the need for a higher vertical resolution over the airport, where the higher resolution can be supported by the data from the TDWR.

Figure 3 shows the data flow for the Terminal Winds cascade-of-scales analysis. First, an analysis is performed with a 10-km horizontal resolution, a 50-mb vertical resolution, and a 30-min update rate utilizing all of the data sources. The 10-km-resolution background field is produced by linear interpolation in space and time between the two RUC forecasts that bracket the analysis time. All data used in the 10-km analysis must have collection times within ninety minutes of the analysis time. The current 10-km analysis is then used as the background wind field for an analysis with a 2-km horizontal resolution, a 50-mb vertical resolution, and a 5-min update rate. Only Doppler radar data and LLWAS data are used in the 2-km analysis. The MDCRS aircraft reports and other surface data are not used in the 2-km analysis because of data latency. On grid levels with no observations, the 2-km analysis is simply the 10-km analysis interpolated to the 2-km-resolution grid.

Wind-Field Analysis from Meteorological Doppler Radar Data

This subsection provides an overview of the basics of winds analysis using information from meteorological Doppler radars. We discuss three topics: (1) data quality, (2) data resampling to produce regionally representative wind estimates on a Cartesian grid from point measurements in spherical coordinates, and (3) estimating horizontal winds from information provided by two or more Doppler radars.

Doppler Radar Errors

Data-quality issues should be addressed before an analysis of the wind field is performed. There are three major types of error in meteorological Doppler radar data:

1. Returns from objects that are not moving with the wind, such as the ground and objects on the ground (ground clutter), or flocks of birds and aircraft (point targets).
2. Velocity values that are misrepresented by velocity folding. These errors result from the insufficient sampling rate in the Doppler velocity calculation. Given a sampling rate, or the pulse repetition frequency (PRF), the unambiguous velocity range is determined by

$$v = \pm \frac{c \cdot \mathrm{PRF}}{4f},$$

where f is the radar frequency and c is the speed of light. When velocity falls outside this range, it is folded back into the range of representable

Table 3. Scales of Analysis for Rapid Update Cycle and Terminal Winds

	Update Rate	*Horizontal Resolution*	*Domain Size*
Rapid Update Cycle	180 min	60 km	national
Terminal Winds above PBL	30 min	10 km	240 x 240 km
Terminal Winds in PBL	5 min	2 km	120 x 120 km

velocities (velocity folding). Both TDWR and NEXRAD have algorithms that attempt to correct for velocity folding.

3. Returns from objects beyond the unambiguous range of the radar. These errors are the result of echoes from distant and bright reflectors, such as large storms or topographic features that are received after a subsequent pulse has been transmitted (multiple trip or range folding).

Currently, the Terminal Winds system does not try to classify radar errors or correct for them. This error detection and correction is performed by each radar system prior to providing data to the ITWS. The Terminal Winds analysis system does attempt to identify incorrect or nonrepresentative wind estimates and remove them during the resampling process.

Radar Data Resampling

Resampling is the process by which radial velocity information is transformed from radar coordinates to

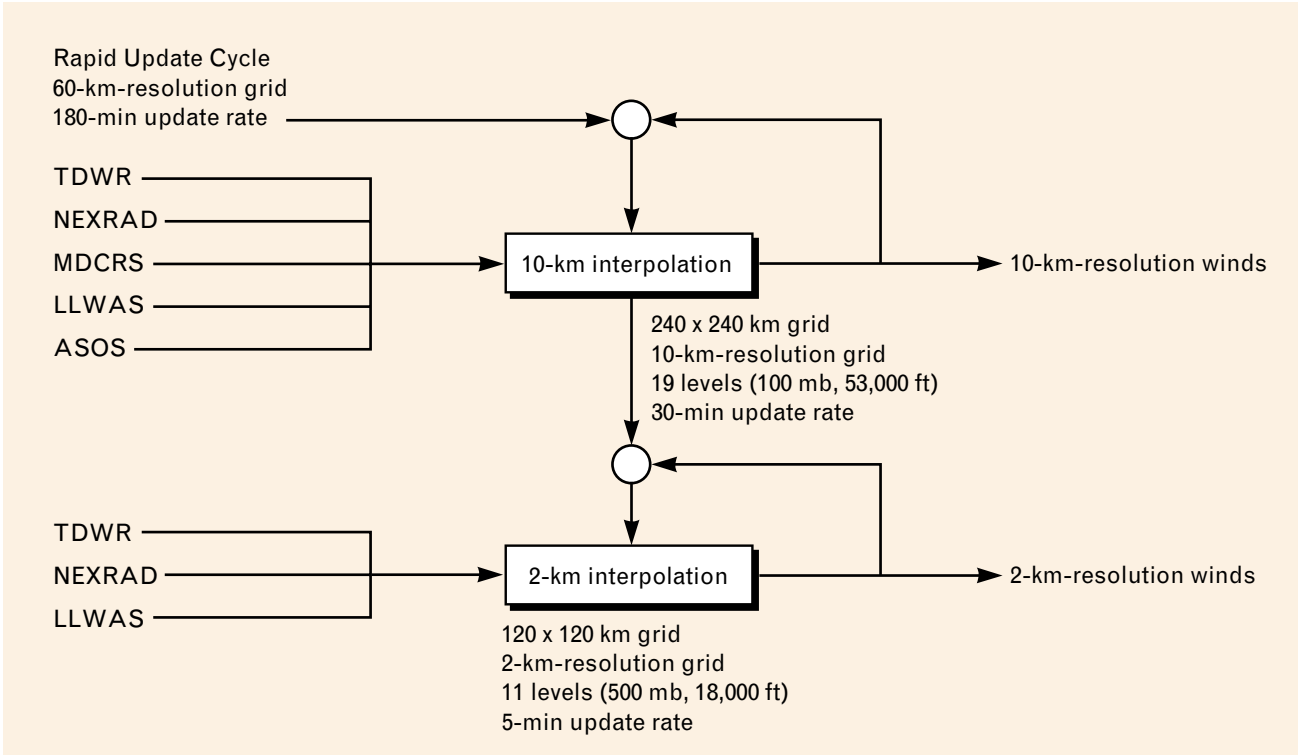

FIGURE 3. Data flow for the Terminal Winds cascade-of-scales analysis. The RUC data are used to initialize an analysis with a 10-km horizontal-resolution grid and a 30-min update rate. The 10-km horizontal-resolution wind field is used in turn to initialize an analysis with a 2-km horizontal-resolution grid and a 5-min update rate. All of the data sources are used in the 10-km analysis, but only Doppler data and LLWAS data are used in the 2-km analysis.

the Cartesian coordinates used in the Terminal Winds analysis. Spatial averaging is used to provide data values that represent a regional average wind. Data-quality tests are used to remove questionable data.

The radar reflectivity and radial velocity data are collected in contiguous, equally spaced gates along each radar beam. Both radars scan sectors of the region with a fixed elevation angle during the scan. A *tilt* is a maximal collection of beams that are contiguous in time and have the same elevation angle. Geometrically, a tilt is a section of a cone whose vertex is at the radar. All NEXRAD tilts are full cones, covering full 360° sectors. NEXRAD has several different scan strategies, each with its own set of tilt elevation angles. TDWR can scan either with 360° sectors (monitor mode), or with two 360° tilts near the surface and an intense pattern of approximately 120° sectors at various elevations over the airport (hazardous-weather mode). The TDWR tilt elevation angles are preset for each airport installation, so there are only two TDWR scan strategies for each airport.

Each radar also interrupts its standard velocity scanning to make long-range (low-PRF) scans that are used to detect the possibility for range folding. The low-PRF data are not used in the winds analysis. They provide an artificial temporal partition of the tilts into volume scans. The Terminal Winds analysis does not make use of this volume structure. Instead, at each analysis time, it composes a volume scan out of the most recent tilts. This design also accommodates the fact that the scan strategies of the radars can change during operations. By constructing its own volume scan from the most recent tilts, the Terminal Winds analysis uses the most current radar data and is able to continue processing during changes in the radar scan strategy.

The resampling of the Doppler radar data is a two-step process—tilt resampling and volume resampling.

Tilt Resampling. This process produces a regionally representative estimate of the radial component of the horizontal wind velocity at each tilt position (x, y, z^*) on an (x, y) column of the analysis grid. The vertical height z^* is the height at which the tilt intersects the (x, y) column of the analysis grid, and does not necessarily correspond to an analysis height z. Each tilt is resampled immediately after its scan is completed, an asynchronous process controlled by the radar scan strategy. The resampled radial velocity for (x, y, z^*) is the median of all tilt data that lie within approximately 0.5 km of (x, y, z^*). A median filter is used instead of a linear filter, because of the possibility of gross data errors such as point targets. Therefore, this step also has a data-quality editing benefit. The radial velocities are corrected to account for elevation angle by assuming that the vertical velocity is zero. The magnitude of the vertical velocity is usually very small except within strongly convective weather. This exception is accounted for in the volume resampling step.

Volume resampling. This process produces a regionally representative estimate of the radial component of the horizontal wind velocity at each analysis position (x, y, z) from the resampled tilts by either linear interpolation or extrapolation in the vertical. This is a synchronous process triggered by each winds-analysis cycle. Additional data-quality editing is provided by (1) a buddy check on each tilt of data to remove questionable data values or data that may not be regionally representative, and (2) removal of data in regions of high reflectivity, since winds within highly convective storms may not be regionally representative and the horizontal wind estimates are likely to be contaminated by a large vertical component.

Multiple-Doppler Techniques

Multiple-Doppler wind-field analysis provides a valuable starting point in the discussion and development of winds-analysis techniques when information from two or more Doppler radars is available. The use of multiple-Doppler radars is the only practical method available for obtaining closely spaced measurements of wind fields in a three-dimensional region. Multiple Doppler analysis can be applied only at points with Doppler information for two independent components of the wind. When Doppler analysis can be applied, however, the resulting wind estimates are very accurate, as discussed below.

The horizontal wind at a point can be estimated from two or more Doppler horizontal wind-component estimates at that location, if the difference in azimuth angles is sufficiently large. Least-squares estimation is usually used for this purpose. This process is numerically stable only if the difference in azimuth

angles is sufficiently large so that the radars have at least two independent estimates of the wind field. Even when the difference in azimuth angles is small, this wind-retrieval process returns one high-quality wind component, the radial component measured by the radars; only the azimuthal component is unstable. Techniques are being developed to estimate the azimuthal component from the motion of features in the reflectivity field. Work in this area is under way at the Cooperative Institute for Mesoscale Meteorological Studies [15] and at the National Center for Atmospheric Research (NCAR) [16]. These azimuthal-component analysis techniques are not used in the current implementation. When these techniques are developed to the point that they can be used operationally, they will be included in the Terminal Winds system as a new source of information.

Multiple-Doppler analysis is the process by which the best estimate of the horizontal wind-velocity vector is computed at an analysis position (x, y, z), on the basis of estimates of the radial velocity produced by resampling the data from two or more Doppler radars. We represent the horizontal wind as a vector (u, v), where u is the component in the east direction and v is the component in the north direction; however, any orthogonal coordinate system can be used. For an azimuth angle θ, with east at 0° and north at 90°, the radar measures a radial velocity r given by

$$r = u \cos\theta + v \sin\theta .$$

Given two or more Doppler wind component estimates, we can write a system of equations with (u, v) as the wind vector to be determined. The system of equations for two Doppler measurements is given by

$$\begin{pmatrix} \cos\theta_1 & \sin\theta_1 \\ \cos\theta_2 & \sin\theta_2 \end{pmatrix} \begin{pmatrix} u \\ v \end{pmatrix} = \begin{pmatrix} r_1 \\ r_2 \end{pmatrix}.$$

To illustrate the mathematical behavior of the solution to the multiple-Doppler system of equations, we consider an example with two Doppler estimates at a point, and simple geometry. Suppose we have two radars, as shown in Figure 4. The radars make measurements r_1 and r_2, respectively, of the radial component of the wind at the intersection of the north and east axes. For small values of θ, the u component of the wind is nearly the radial component and the v component is nearly the azimuthal component. The radar measurement contains little information about v. Similar geometry can always be arranged by using a rotation of coordinates to choose a suitable coordinate system, as shown in Figure 5.

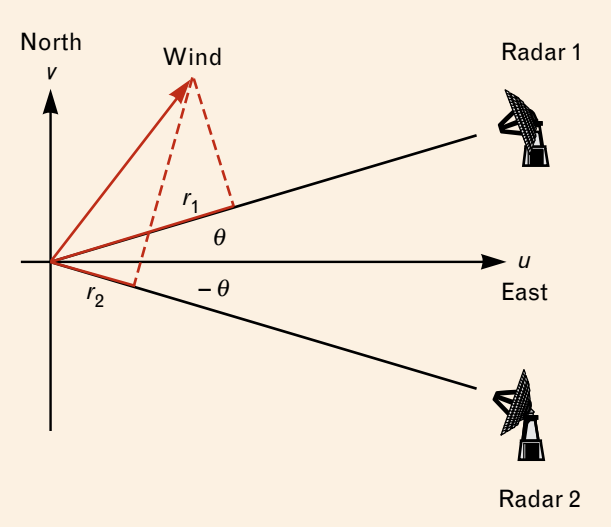

FIGURE 4. Simple geometry for two Doppler radars. Each radar makes a measurement of the wind at the intersection of the north and east axes. For small values of θ, the u component is nearly the radial component, and the radar measurement contains little information about v.

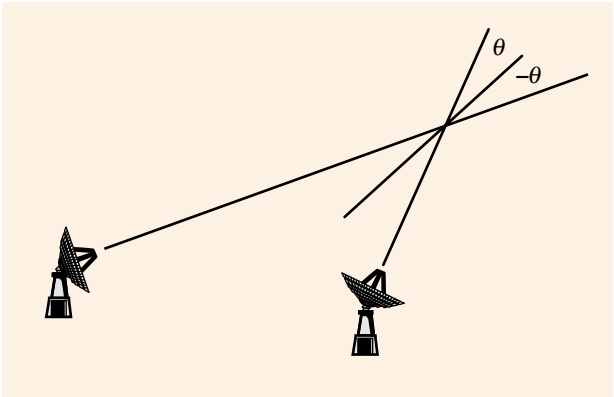

FIGURE 5. General geometry for two Doppler radars. The measurement geometry shown in Figure 4 can always be created by performing a rotation of coordinates into a suitable coordinate system.

The dual-Doppler equations for the simple geometry of Figure 4 are

$$\begin{pmatrix} \cos\theta & \sin\theta \\ \cos\theta & -\sin\theta \end{pmatrix} \begin{pmatrix} u \\ v \end{pmatrix} = \begin{pmatrix} r_1 \\ r_2 \end{pmatrix}. \quad (1)$$

The solution to Equation 1 is

$$\begin{pmatrix} u \\ v \end{pmatrix} = \begin{pmatrix} (r_1 + r_2)/2\cos\theta \\ (r_1 - r_2)/2\sin\theta \end{pmatrix}.$$

Let u_{eDD} and v_{eDD} denote the error in the u and v components of the dual-Doppler solution. Let σ_R^2 denote the average of the error variances for the two radars. The dual-Doppler error variances, provided that the radars have uncorrelated errors, are

$$\text{var}(u_{eDD}) = \frac{\sigma_R^2}{2\cos^2\theta}$$

and

$$\text{var}(v_{eDD}) = \frac{\sigma_R^2}{2\sin^2\theta}.$$

As θ approaches zero, the error in the solution for v becomes numerically unstable. To control this numerical instability, the angle between radar beams, 2θ, is generally constrained to be greater than 30°. Figure 6 shows the region where 2θ is greater than 30° for a TDWR/NEXRAD dual-Doppler analysis at the Lincoln Laboratory testbed in Orlando.

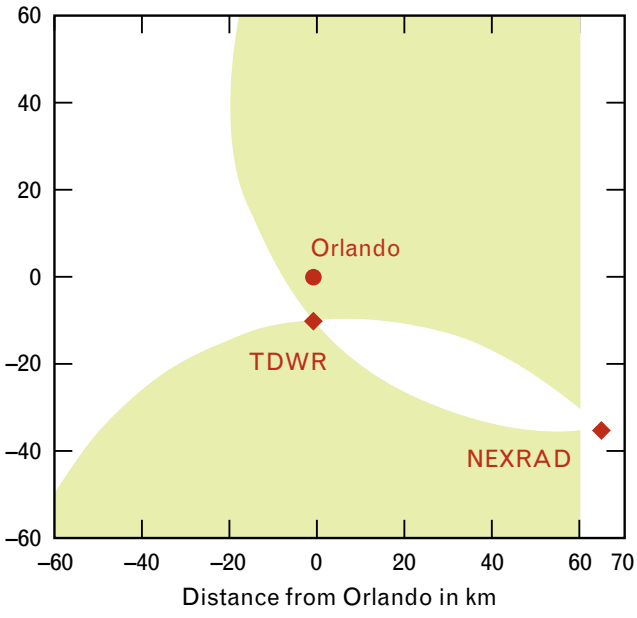

FIGURE 6. The shaded region depicts the numerically stable TDWR/NEXRAD dual-Doppler region for the Orlando airport overlaid on the 2-km-resolution analysis domain.

We now consider the general case of multiple Doppler radars. Figure 7 shows an example of a situation in which a given location is covered by three Doppler radars. In this case the Doppler equations are

$$\begin{pmatrix} \cos\theta_1 & \sin\theta_1 \\ \cos\theta_2 & \sin\theta_2 \\ \cos\theta_3 & \sin\theta_3 \end{pmatrix} \begin{pmatrix} u \\ v \end{pmatrix} = \begin{pmatrix} r_1 \\ r_2 \\ r_3 \end{pmatrix}, \text{ or } \mathbf{A}\begin{pmatrix} u \\ v \end{pmatrix} = \begin{pmatrix} r_1 \\ r_2 \\ r_3 \end{pmatrix}.$$

The best-estimate solution is provided by least squares, given by

$$\begin{pmatrix} u \\ v \end{pmatrix} = (\mathbf{A}^T\mathbf{A})^{-1}\mathbf{A}^T \begin{pmatrix} r_1 \\ r_2 \\ r_3 \end{pmatrix}.$$

Even though this system of equations is overdetermined, it is not numerically stable unless at least two of the angles are significantly different.

In this formulation of the least-squares problem, each radar is treated as if it produced radial measurements of equal quality. However, many factors can introduce unequal errors in the data, such as radar sensitivity or the distance from the radar site to the analysis location. In our wind-field analysis, unequal errors are accounted for by means of the Gauss-Markov theorem [17].

Terminal Winds Interpolation Technique: Optimal Estimation

The Local Analysis and Prediction System (LAPS), developed by NOAA/FSL, provided the basis for the initial Terminal Winds prototype. In 1992, LAPS was the state-of-the-art operational 10-km-resolution winds-analysis system for fusing data from Doppler radars as well as traditional wind-data sources, numerical models, anemometers, MDCRS, and other meteorological data sources. However, while LAPS can utilize data from more than one Doppler radar, it

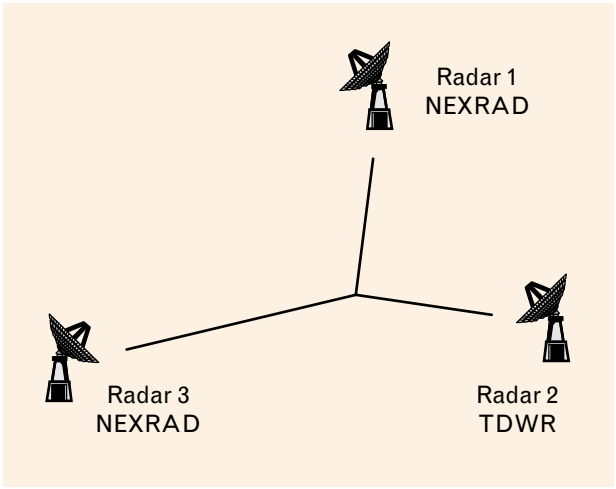

FIGURE 7. Radar geometry for the overdetermined case of three Doppler radars.

was not designed to take advantage of the large multiple-Doppler data sets available in an ITWS. This initial Terminal Winds prototype was demonstrated in real time in the Lincoln Laboratory Orlando testbed in the summers of 1992 and 1993. The operation of this prototype, as well as numerous discussions with FSL, provided valuable insight into traditional winds-analysis techniques. The initial prototype has been superseded by the Terminal Winds analysis described in this article.

The Terminal Winds analysis is dominated by Doppler radar data. In regions with coverage by two or more radars, the Terminal Winds analysis system should provide information about winds with at least the quality of the information from the multiple-Doppler analysis discussed earlier. The state-of-the-art analysis technique for non-Doppler meteorological data analysis is optimal interpolation [18, 19], which is a statistical interpolation technique that under certain hypotheses gives an unbiased minimum-variance estimate. In other scientific fields, similar minimum-variance techniques have been used successfully. In geophysics a technique called Kriging, which is similar to optimal interpolation, is used [20], and in oceanography optimal interpolation is called the Gauss-Markov method [21]. We wish to build on the foundation laid down by the multiple-Doppler analysis and by these other statistical interpolation techniques.

We have developed a minimum-variance technique that utilizes Doppler measurements directly. We call this technique optimal estimation to distinguish it from optimal interpolation. The initial focus is on analyzing horizontal wind data in a three-dimensional grid; however, the method also applies to other weather variables such as temperature and humidity. The method is based on the Gauss-Markov theorem, and under suitable conditions gives an unbiased minimum-variance estimate of the horizontal winds. Optimal estimation is an extension of both optimal interpolation and multiple-Doppler analysis. The development of optimal estimation is motivated by the ease with which it incorporates Doppler radar data. Because our software development lags behind our theoretical understanding of optimal estimation, we present only that part of optimal estimation which has been tested, leaving a full treatment to a later time.

Optimal estimation has the following properties: (1) dual-Doppler-quality winds are automatically provided in regions where dual Doppler is numerically stable, (2) small gaps in dual-Doppler radar coverage are filled to provide near dual-Doppler-quality winds in these gaps, and (3) the analysis produces wind vectors that vary smoothly between regions with data from differing numbers of Doppler radars.

Throughout this section we use the following notation conventions: r denotes a radial wind component, u denotes an east wind component, v denotes a north wind component, superscript a denotes an analyzed quantity, superscript b denotes a background quantity, superscript o denotes an observed quantity, and subscripts denote location (o denoting an analysis location).

We seek a linear minimum-variance unbiased estimate, and we employ the Gauss-Markov theorem to generate this estimate. To apply the Gauss-Markov theorem we need to pose the problem in the form

$$\mathbf{A}\mathbf{x} = \mathbf{d}\,, \tag{2}$$

where

$$\mathbf{x} = \left(u_0^a, v_0^a\right)^T\,,$$

and the data vector

$$\mathbf{d} = \left(u_o^b, v_o^b, u_1^o, v_1^o, \ldots, u_m^o, v_m^o, r_1^o, \ldots, r_n^o\right)^T$$

contains the background estimate at the analysis location and observations in a data window centered on the analysis location. The form of the matrix **A** depends on the type of data, vector, or radial to be analyzed. The Gauss-Markov theorem states that the linear minimum-variance unbiased estimate of **x** is given by

$$\mathbf{x} = \left(u_0^a, v_0^a\right)^T = \left(\mathbf{A}^T\mathbf{C}^{-1}\mathbf{A}\right)^{-1}\mathbf{A}^T\mathbf{C}^{-1}\mathbf{d}, \qquad (3)$$

if each element of **d** is unbiased, and **C** is the error covariance matrix for the elements of **d**. The error covariance of the solution is

$$\left(\mathbf{A}^T\mathbf{C}^{-1}\mathbf{A}\right)^{-1}. \qquad (4)$$

In the case of *m* vector observations and *n* Doppler observations, Equation 2 has the form

$$\begin{pmatrix} 1 & 0 \\ 0 & 1 \\ \vdots & \vdots \\ 1 & 0 \\ 0 & 1 \\ \cos\theta_1 & \sin\theta_1 \\ \vdots & \vdots \\ \cos\theta_n & \sin\theta_n \end{pmatrix} \begin{pmatrix} u_o^a \\ v_o^a \end{pmatrix} = \begin{pmatrix} u_o^b \\ v_o^b \\ \vdots \\ u_m^o \\ v_m^o \\ r_1^o \\ \vdots \\ r_n^o \end{pmatrix}$$

Unlike the multiple-Doppler analysis, the optimal-estimation solution is always numerically stable because of the inclusion of the background wind estimate. The inclusion of a (u_o^b, v_o^b) data point provides two component estimates at right angles, giving a maximum spread of azimuth angles. Since the error variances of the Doppler data are usually much smaller than the error variances of the other data, the optimal-estimation solution closely matches the multiple-Doppler solution at locations where the multiple-Doppler problem is well conditioned. Otherwise, the analysis gives a solution that largely agrees with the radar observations in the radial component measured by the radars. The remaining component is derived from the non-Doppler data sources. An example illustrating this feature is given in the next section.

In practice, the error covariance matrix **C** is not known and must be estimated. There are two types of errors to estimate. The first is the error that arises from imperfect sensors. The second is the displacement error due to taking the measurement at some distance, in space and time, from the analysis location. Our initial error models are based on the following simplifying assumptions: (1) observations are unbiased; (2) sensor errors from different observations are uncorrelated; (3) errors in *u* and *v* components, measured or background, are uncorrelated; (4) displacement errors and sensor errors are uncorrelated; and (5) displacement errors are independent of the component being measured.

With these assumptions, the error covariance matrix **C** decomposes into the sum of a sensor-error covariance matrix and a displacement-error covariance matrix. The sensor-error covariance matrix is diagonal, and the sensor-error variances are known. The remaining task is the estimation of the displacement-error covariance matrix.

The initial displacement-error variance model is a linear function of the displacement between the observation location and the analysis location. The initial displacement-error correlation model for two like components is a decreasing exponential function of the displacement between two observation locations. The displacement-error covariance model for two nonorthogonal, nonparallel components must take into account the angle between the two components. We denote the angle between the observed component and the *u* axis by θ, with east at 0° and north at 90°, and the displacement error in observation *i* by δ_i^o. Then the displacement-error covariance for two observations is given by the following equation:

$$\begin{aligned}&\operatorname{cov}(\delta_1^o, \delta_2^o)\\ &\quad = \cos(\theta_1 - \theta_2)\sqrt{\operatorname{var}(\delta_1^o)\operatorname{var}(\delta_2^o)}\,\operatorname{cor}(\delta_1^o, \delta_2^o),\end{aligned}$$

where $\operatorname{cor}(\delta_1^o, \delta_2^o)$ is the displacement-error correlation model.

Illustrative Examples

We illustrate some benefits of optimal estimation by applying it in two examples for which solutions are easily computed. The first example demonstrates some advantages of the optimal estimation technique over the standard dual-Doppler technique. The second illustrates the benefit of accounting for correlated errors that arise from nonuniform data distributions. The ability to account for correlated errors is especially important for a system that utilizes Doppler information because the Doppler data are often not uniformly distributed throughout the analysis domain.

For our first example, we compare optimal-estimation analysis to dual-Doppler analysis at those points with coverage from two radars. We restrict our discussion to the case in which we have only a background wind estimate and two Doppler observations at a fixed analysis location, as illustrated in Figure 4.

We use the assumptions listed above regarding the error models. That is, we assume the errors in the u and v components of the background are not correlated with each other or with the error in the radar measurements, and we assume that the errors in the radar measurements are not correlated. We also assume that the error variance is the same for each component of the background wind, and that the error variance is the same for each radar. These are reasonable assumptions if the Doppler values are average (or median) values over a fixed region surrounding the analysis point, and the background is independent of the Doppler data. The background is independent of the Doppler data, for example, if the background comes from a forecast model or is derived from the radar reflectivity fields. Let σ_B be the standard deviation of the error in the background components, and let σ_R be the standard deviation of the error in the radar measurements. This gives the error correlation matrix $\mathbf{C}$, where

$$\mathbf{C} = \begin{pmatrix} \sigma_B^2 & 0 & 0 & 0 \\ 0 & \sigma_B^2 & 0 & 0 \\ 0 & 0 & \sigma_R^2 & 0 \\ 0 & 0 & 0 & \sigma_R^2 \end{pmatrix}.$$

Let $\rho = \sigma_B^2 / \sigma_R^2$ denote the relative quality of the radar observations versus the background observations. Typically, ρ is on the order of 10. Then

$$\mathbf{C}^{-1} = \frac{1}{\sigma_B^2} \begin{pmatrix} 1 & 0 & 0 & 0 \\ 0 & 1 & 0 & 0 \\ 0 & 0 & \rho & 0 \\ 0 & 0 & 0 & \rho \end{pmatrix}.$$

With these assumptions, the optimal-estimation solution is computed from Equation 3, giving:

$$u_o^a = \alpha u_o^b + (1 - \alpha) \frac{r_1^o + r_2^o}{2 \cos\theta}$$

and

$$v_o^a = \beta v_o^b + (1 - \beta) \frac{r_1^o - r_2^o}{2 \sin\theta},$$

where

$$\alpha = \frac{1 + 2\rho \sin^2\theta}{1 + 2\rho + 4\rho^2 \cos^2\theta \sin^2\theta}$$

and

$$\beta = \frac{1 + 2\rho \cos^2\theta}{1 + 2\rho + 4\rho^2 \cos^2\theta \sin^2\theta}.$$

The terms $1-\alpha$ and $1-\beta$ represent the fraction of the optimal-estimation solution that is given by the solution to the dual-Doppler equations for the u and v components. If α or β is zero, the corresponding component of the optimal-estimation solution is equal to the dual-Doppler solution, and if α or β is 1, the corresponding component of the optimal-estimation solution is equal to the background estimate.

We see that if ρ is large (i.e., the radar error variance is small relative to the error variance of the background) and θ is not near zero, then α and β are near zero, and the optimal-estimation solution is nearly dual Doppler. If $\theta = 0$, then $\beta = 1$, and optimal estimation returns a v component equal to the background. In this last case, the u component is the stan-

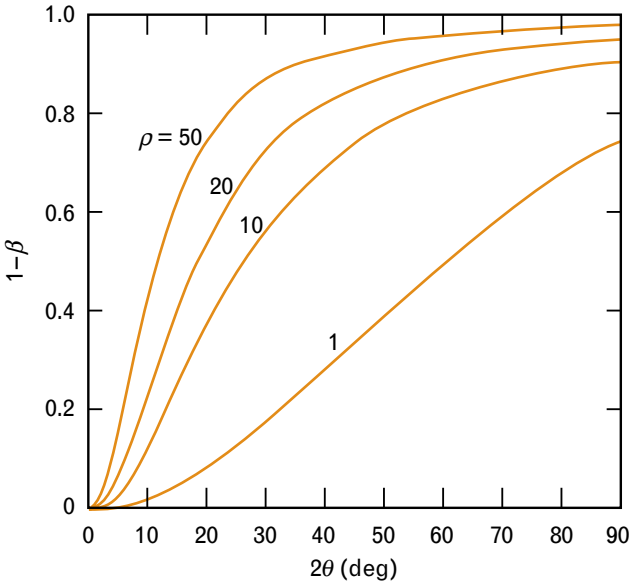

FIGURE 8. The fractional contribution of the dual-Doppler term in the optimal-estimation solution of the v component, as a function of the angle between radar beams (2θ) and the quantity ρ, which is a measure of the relative quality of the radar observations. If ρ is large and θ is not near zero, the optimal-estimation solution for v is primarily the dual-Doppler solution. If θ is near zero, the dual-Doppler contribution drops to zero.

dard least-squares solution; the background and Doppler values are weighted inversely to their variances. Figure 8 shows how $1-\beta$ varies with the angle between the two radar beams (2θ) for different values of ρ. When the angle is greater than about 30°, optimal estimation returns a value for v that is primarily the dual-Doppler solution. As the angle decreases below 30°, the weight given to the v component of the dual-Doppler solution drops quickly to zero. In fact, as θ decreases to zero, the quantity

$$(1-\beta)\frac{r_1^o - r_2^o}{2\sin\theta}$$

goes to zero, removing the dual-Doppler instability for small θ.

The error variances for the optimal-estimation solution, computed from Equation 4, are

$$\mathrm{var}(u_{eOE}) = \frac{\sigma_B^2}{1 + 2\rho\cos^2\theta} \tag{5}$$

and

$$\mathrm{var}(v_{eOE}) = \frac{\sigma_B^2}{1 + 2\rho\sin^2\theta}, \tag{6}$$

again demonstrating the numerical stability of the method; the error variance of the optimal-estimation solution is bounded above by the error variance of the background.

Substitution of $\rho = \sigma_B^2 / \sigma_R^2$ into Equations 5 and 6 gives

$$\mathrm{var}(u_{eOE}) = \frac{\sigma_B^2\sigma_R^2}{\sigma_R^2 + 2\sigma_B^2\cos^2\theta} \le \frac{\sigma_B^2\sigma_R^2}{2\sigma_B^2\cos^2\theta} = \frac{\sigma_R^2}{2\cos^2\theta} \tag{7}$$

and

$$\mathrm{var}(v_{eOE}) = \frac{\sigma_B^2\sigma_R^2}{\sigma_R^2 + 2\sigma_B^2\sin^2\theta} \le \frac{\sigma_B^2\sigma_R^2}{2\sigma_B^2\sin^2\theta} = \frac{\sigma_R^2}{2\sin^2\theta}. \tag{8}$$

These equations show that the error variances of the optimal-estimation solution are never greater than the error variances of the dual-Doppler solution. Combining Equations 5 through 8, we conclude that

$$\mathrm{var}(u_{eOE}) \le \min\{\mathrm{var}(u_{eDD}), \mathrm{var}(u_{eB})\}$$

and

$$\mathrm{var}(v_{eOE}) \le \min\{\mathrm{var}(v_{eDD}), \mathrm{var}(v_{eB})\}.$$

In the second example we look at an important benefit of statistical methods such as optimal interpolation and optimal estimation—namely, their ability to handle correctly situations with a significant spatial variation in the density of observations, resulting in observations with highly correlated displacement errors. For simplicity, we examine an example with a single variable, and we omit a background estimate. Figure 9 shows an example with three observations. We assume that the sensor errors are equal and uncorrelated. Observation 1 is located far from observa-

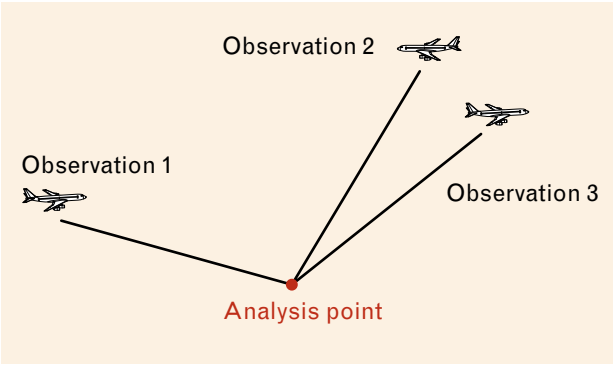

FIGURE 9. Nonuniform data distribution gives rise to correlation errors. Observation 1 is located far from observations 2 and 3, so its displacement error is nearly uncorrelated with the displacement errors in the other two observations, which are close together and are highly correlated. The statistical analysis methods of optimal interpolation and optimal estimation account for the error correlations caused by this distribution.

tions 2 and 3; therefore, its displacement error is nearly uncorrelated with the displacement errors in the other two observations. To simplify the example, we assume the displacement error in observation 1 is uncorrelated with the displacement errors in observations 2 and 3. Observations 2 and 3, on the other hand, are located close together, so we assume that their displacement errors are highly correlated. Observations 2 and 3 are nearly repeat observations, and as such they should not get twice the weight of a single independent observation, as is the case when error correlations are not accounted for.

Because the observations are equidistant from the analysis point, we assume that their displacement error variances are equal, and without loss of generality we assume that the sum of the sensor-error variance and the displacement-error variance is equal to one for each observation. Since we have assumed that the errors in observation 1 are uncorrelated with the errors in observations 2 and 3, the error covariance matrix **C** has the following form:

$$\mathbf{C} = \begin{pmatrix} 1 & 0 & 0 \\ 0 & 1 & c_{23} \\ 0 & c_{23} & 1 \end{pmatrix},$$

where $0 \le c_{23} < 1$. The entry c_{23} cannot equal one because the sensor errors are uncorrelated.

To compute the optimal-estimation solution, we invert **C** and apply Equation 3, with $\mathbf{A} = (1 \quad 1 \quad 1)^T$. Examination of the weight of each observation gives

$$w_1 = \frac{1 + c_{23}}{3 + c_{23}}, \quad w_2 = w_3 = \frac{1}{3 + c_{23}}.$$

We see that if the errors are assumed to be uncorrelated (i.e., the error correlations are not accounted for), the observations each get weight 1/3. As c_{23} increases toward 1, the weight given to observation 1 increases toward 1/2, and the weights given to observations 2 and 3 decrease toward 1/4, or a combined weight of 1/2. This is the desired weighting because if the errors in observations 2 and 3 are completely correlated, observations 2 and 3 contain the same information.

Operational Experience and Evaluation

Starting in 1992, Lincoln Laboratory has operated an ITWS testbed at Orlando International Airport. This testbed is a continuation of the Lincoln Laboratory TDWR testbed that was initiated in 1990. In the summers of 1992 and 1993 the initial Terminal Winds prototype operated in real time, and in the summer of 1993 the new optimal-estimation-based Terminal Winds prototype operated in real time. The evaluation results presented here are from data collected in 1992 and 1993 at the Orlando testbed.

The wind-data sources in the Orlando testbed are the Mesoscale Analysis and Prediction System (MAPS), which is a prototype of the RUC system; the TDWR prototype Doppler radar at Kissimmee, Florida, 10 km south of Orlando; the NEXRAD Doppler radar at Melbourne, Florida, 65 km southeast of Orlando; MDCRS-equipped aircraft observations; the LLWAS anemometer network; the ASOS automatic observing stations; and Surface Aviation Observations (SAO) hourly observations.

The Doppler radars complete their volume scans every five to six minutes. The ASOS stations provide updates every twenty minutes, and the LLWAS anemometers provide updates every ten seconds. The LLWAS network is located at the airport and contains fourteen sensors with a spacing of 2 to 3 km. The SAOs are updated on the hour. The MDCRS reports occur with variable spacing, averaging about ten per

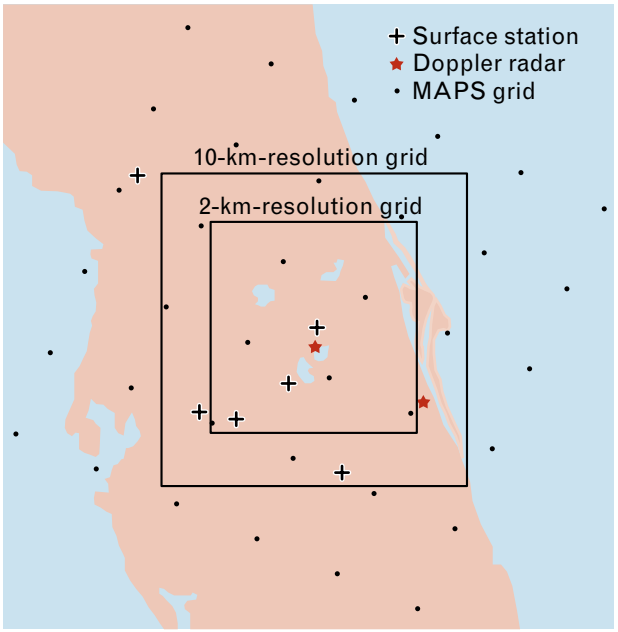

FIGURE 10. Analysis domains and sensor locations for the 1992 Orlando Terminal Winds analysis. The 180 x 180-km analysis region (10-km-resolution grid) and the 120 x 120-km analysis region (2-km-resolution grid) are shown as squares centered on the airport.

hour during the hours of peak aircraft operation.

Figure 10 shows the analysis domains and sensor locations for the 1992 Orlando Terminal Winds analysis. The 10-km and 2-km analysis regions are shown as squares centered on the airport. The dimensions are 180 km × 180 km and 120 km × 120 km, respectively. In 1993 the 10-km analysis region was increased to 240 km × 240 km. The background field for the 10-km analysis was derived from the wind estimates on the 6 × 6 sub-domain of the MAPS grid that contains the 10-km-resolution grid. The TDWR radar is located near the center of the 2-km domain, and the NEXRAD radar is located near the southeast corner of the 2-km domain. Aircraft reports were available primarily along arrival and departure routes, to the north and south of the airport.

The basis of the evaluation is the comparison of observations with analyzed and forecast winds at nearly coincident points. This amounts to spot checks, since we cannot control the availability of observations, except to select days on which they were plentiful. Each algorithm was evaluated on a twenty-day subset of the 1992 and 1993 Orlando data archive. These days were chosen to include a variety of weather, and good comparison data.

Statistics for a number of performance metrics have been compiled. We report statistics only for the norm of the vector difference between the analyses and forecasts and the comparison observations. Three comparison observation data sets were used—MDCRS reports, Cross-Loran Atmospheric Sounding System (CLASS) soundings, and TDWR and NEXRAD dual-Doppler wind fields. These comparison data sets are discussed in detail below.

Results are presented for two analyses and one forecast: Terminal Winds 2-km resolution, Terminal Winds 10-km resolution, and MAPS. Comparisons between analyzed and forecast wind fields and observed winds were constrained to the 2-km grid to ensure consistent evaluation data sets and because product accuracy is paramount in this region. We used bilinear interpolation of the Terminal Winds 10-km analyses and MAPS forecasts to the 2-km grid. For each analysis, the observations were compared to the wind vector from the 2-km grid point nearest the observation.

Although each of the three comparison data sets is treated as a standard against which the analyzed wind fields are judged, it is important to keep in mind that no observation is perfect. The performance of each algorithm is referred to as "relative to MDCRS," for example, keeping explicit that any conclusions we draw are subject to the error characteristics of the comparison observations, as well as the error characteristics of the analysis. We cannot expect the comparison with independent observations, on average, to be less than the average magnitude of the sensor error. This limits the ability of the comparison to discern product accuracy to the accuracy of the comparison observations.

The characterization of a "perfect" local winds analysis has not been made. In particular, the desired degree of smoothing of the wind field has not been specified. At any given instant, a wind field is a superposition of wind structures with a wide spectrum of spatial and temporal scales. For a given application, some of these structures are at scales that are unimportant, and other structures are too small or short lived to be captured by the analysis. These subscale

features may influence an observation, however. When these observations are compared with the analysis, the differences reflect errors in the analysis, errors in the observation, and the structure of the subscale features captured in the observations. Given the limited set of observations used in the evaluation, we have not attempted to separate the effects of the different sources of error.

Comparison Observation Data Sets

There are three types of comparison observations used in the evaluation. Two of these—MDCRS observations and CLASS soundings—are independent of the associated analysis fields. The independence of MDCRS is explained in the next paragraph. The third type of comparison observation—dual-Doppler winds based on TDWR and NEXRAD—is not independent of the analyzed wind fields because both the Terminal Winds analysis and the dual-Doppler analysis are derived from the same Doppler radar data, including similar data-quality editing.

Despite the fact that MDCRS observations are inputs to the analysis, they are independent of the analyzed wind fields to which they are compared. The MDCRS observations are used as inputs to the 10-km analysis, but are always at least fifteen minutes old by the time they are assimilated. MDCRS-observed winds are compared with the corresponding analysis winds at the analysis update time closest to the MDCRS measurement time, not the MDCRS assimilation time. This time delay results in comparing the MDCRS observation to an analysis computed before the MDCRS report was available to the Terminal Winds system. MDCRS observations are quite sparse in space and time (approximately five per hour in the 2-km analysis domain in which the evaluation was performed). They offer the advantage that they are located where aircraft operate and thus are relevant to air traffic concerns. Preliminary results from a study conducted by the NOAA FSL indicate that MDCRS observations have an rms vector error of approximately 4 m/sec.

Table 4. Height Distribution for the Three Observational Data Sets

	Level (mb)	*Nominal Altitude MSL (feet)*	*Observational Data Set*		
			MDCRS	CLASS	Dual Doppler
	500	18,290	4	9	0
	550	15,960	79	7	29k
	600	13,800	61	10	31k
Sample	650	11,780	87	9	27k
Size	700	9880	104	10	25k
per	750	8090	98	12	31k
Level	800	6390	52	12	30k
	850	4780	63	10	22k
	900	3240	91	10	77k
	950	1770	96	11	337k
	1000	360	0	4	3k
	Totals		735	104	612k

The University of Massachusetts–Lowell launched CLASS rawinsondes during August 1992 from the University of North Dakota radar site located slightly east of the Orlando airport. Several soundings had to be omitted because of poor data quality or because of balloon position alignment errors. For the evaluation, seven CLASS soundings were judged acceptable, representing seven vertical profiles with a total effective sample size of roughly one hundred data points. The accuracy of rawinsonde wind-speed observations, measured by rms error, is typically 3 m/sec. For wind direction, the accuracy is typically 14° when the true wind speed exceeds 5 m/sec [22].

When two Doppler measurements exist at a given location, a wind vector can be reliably recovered from the two measured components, assuming certain geometrical constraints are satisfied. The dual-Doppler computations were performed only in regions where the angle between the TDWR and NEXRAD radar beams is greater than 30° and less than 150° to avoid numerical instability. Data from high-reflectivity regions were additionally eliminated, since wind-velocity variations in convective weather make it difficult to characterize a 2-km cell by a single representative value. Also, the interpolation and extrapolation limits in the volume resampler were reduced by a factor of two to reduce errors introduced during the transformation from radar coordinates to Cartesian coordinates. Finally, no tilts with elevation angle above 20° were used in order to limit the error from sampling the vertical component of the wind. We do not have a sufficiently accurate set of wind measurements to establish the accuracy of our dual-Doppler winds empirically; however, theoretical arguments show that the rms vector error is approximately 2.4 m/sec.

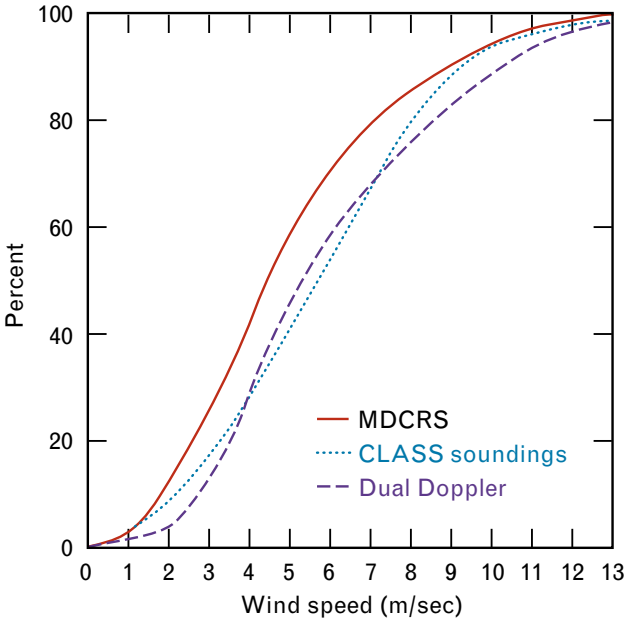

FIGURE 11. Cumulative probability distribution for wind speeds in the MDCRS, CLASS soundings, and dual-Doppler analysis data sets.

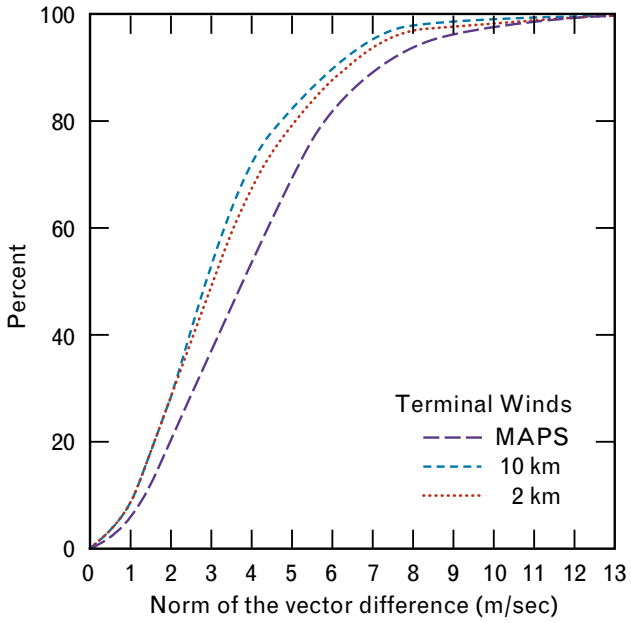

FIGURE 12. Cumulative probability distribution for the norm of the vector difference between the MDCRS reports and each of the three sets of wind fields.

Table 4 shows the height distribution for the MDCRS, CLASS soundings, and dual-Doppler analysis data sets. Both MDCRS and CLASS are fairly uniformly distributed in altitude. The dual-Doppler wind vectors are fairly uniformly distributed in altitude above 4000 feet, with a significant abundance closer to the ground. Only a few dual-Doppler wind vectors are at 1000 mb because of a very small region of overlap in radar coverage at this altitude. Figure 11 gives the cumulative probability distribution for wind speeds of the observations in the three comparison data sets. For example, Figure 11 shows winds speeds of 5 m/sec or less for approximately 57% of the MDCRS data, 40% of the CLASS soundings data, and 45% of the dual-Doppler wind vectors.

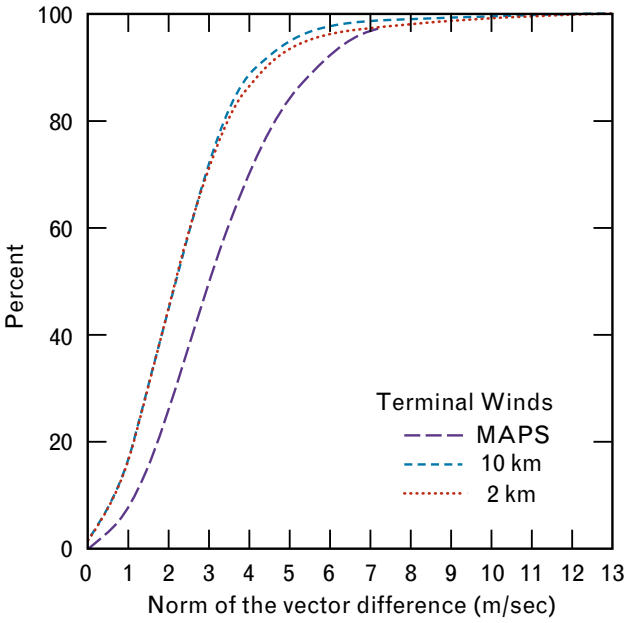

FIGURE 13. Cumulative probability distribution for the norm of the vector difference between the CLASS soundings and each of the three sets of wind fields.

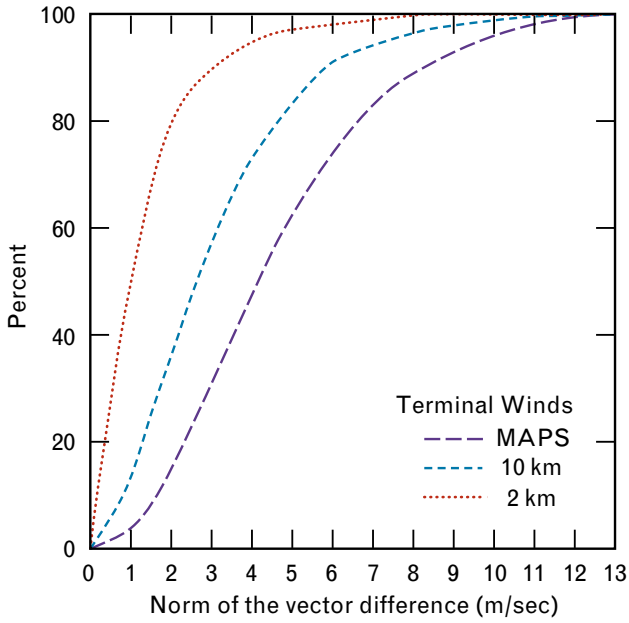

FIGURE 14. Cumulative probability distribution for the norm of the vector difference between the dual-Doppler analysis and each of the three sets of wind fields.

Evaluation Results

The statistical evaluation indicates how well the Terminal Winds algorithm matches the comparison observations over a large period of time. Statistics collected over a large period of time do not allow performance quantification for different weather situations. For example, when the winds are relatively uniform, a 2-km analysis is not expected to perform better than a 10-km analysis, since the wind field does not contain structures smaller than tens of kilometers. When the wind fields are more complex, we expect to see a variation in performance.

The comparison with dual-Doppler observations did not target specific weather situations; however, the majority of the dual-Doppler observations are in the PBL, and they are more numerous in regions of moderate reflectivity. Complex wind fields are expected in the PBL and during convection, so the results of the comparison with dual Doppler are indicative of algorithm performance when small-scale wind features are present in the atmosphere. In addition, we discuss an example in the next section that qualitatively indicates the differences in the two scales of analysis during convection.

Unlike dual Doppler, the presence of MDCRS and CLASS observations is not correlated with the type of weather. These data sets are too small to be partitioned by weather type, so the results of the comparison with MDCRS and CLASS represent an average over all the weather situations occurring during MDCRS and CLASS data collection.

Figures 12, 13, and 14 are plots of cumulative probability distributions for the norm of the vector difference between each analysis and forecast, and each of the three sets of comparison observation data sets. For example, Figure 12 shows that the vector difference between MAPS forecasts and MDCRS is 5 m/sec or less about 70% of the time. Table 5 gives the RMS and median values for the norm of the vector differences between the analyses and forecasts, and the comparison observations.

Figures 12 and 13 provide the comparisons of the Terminal Winds analyses and the MAPS forecasts to MDCRS and CLASS observations, respectively. These comparisons (summarized in Table 5) indicate that both the 2-km and 10-km analyses consistently have better agreement with the observations than do the MAPS forecasts. These comparisons do not indicate that the 2-km analysis provides an improvement

Table 5. Root Mean Square and Median (in Parentheses) Values for the Norm of the Vector Difference between the Terminal Winds Analyses and MAPS Forecasts, and the Three Comparison Observations (m/sec)

	2 km	*10 km*	*MAPS*
MDCRS	4.1 (3.1)	3.8 (2.8)	4.6 (3.6)
CLASS	2.9 (2.2)	2.7 (2.2)	3.7 (3.0)
Dual Doppler	2.0 (1.0)	3.8 (2.6)	5.4 (4.1)

over the 10-km analysis. This result is not too surprising, since these comparisons are over all weather situations. The similarity in performance of the two scales of analysis may also reflect that we have reached the limit of these data sets to discern algorithm performance. Against MDCRS, the two analyses have approximately a 4 m/sec rms error, and against CLASS they have approximately a 3 m/sec rms error, which are the reported RMS accuracies of the MDCRS and CLASS observations. The wind fields, including MAPS forecasts, agree more closely with the CLASS soundings than with the MDCRS reports. This closer agreement may be due to superior accuracy of the CLASS sounding measurements, or it may be due to the expected variation in the statistics when small data sets are used.

The comparison with the dual-Doppler winds analysis provides greater distinction between the various analyses; the 2-km analysis matches the dual-Doppler winds more closely than the 10-km analysis. The rms vector difference between the 2-km analysis and the dual-Doppler wind vectors (as shown in Table 5) is less than the theoretical rms vector error of the dual-Doppler winds (2.4 m/sec), reflecting the statistical dependence between the two estimates of the wind field. Both the 2-km and 10-km Terminal Winds analyses show a greater improvement over MAPS forecasts than they show in the comparisons to MDCRS. This improvement is expected. The dual-Doppler data set contains observations from more complex wind fields than the other two comparison data sets, since the Doppler data are dominated by observations in the PBL, and relatively more Doppler returns are available during and near convective weather than in weather with more clear air. Thus the dual-Doppler data set contains observations in regions where MAPS is not expected to perform well. The relationship between the optimal-estimation algorithm and the dual-Doppler algorithm is also in evidence. Because care was taken to ensure that dual-Doppler winds were produced only when good Doppler data were available, and only in regions where the dual-Doppler process is numerically stable, the ability to match the dual-Doppler winds is important.

An Example

The bulk statistics reported above address the question of how the different analyses perform on average. However, there are differences in the analyses that are not explored by this type of evaluation. In this section we give an example that shows the ability of the different winds analyses to capture important small-scale wind-field structures. We discuss the 2-km-resolution and 10-km-resolution Terminal Winds analyses and MAPS forecast fields for two time periods on the afternoon of 20 August 1992. The behavior discussed is typical for convective weather situations.

Each figure discussed in this example shows an analyzed wind field at approximately 1800 feet MSL in the region covered by the 2-km analysis. Each wind field is displayed on a 4-km-resolution grid to aid the comparison. The 4-km grid was chosen to avoid visual clutter. The wind vectors are scaled to wind speed, with a 5-m/sec reference vector shown in the upper right corner. The Orlando airport is at the center of the wind field, the coast of Florida is shown along the right, and the outlines of four lakes are shown. The colored background indicates the radar reflectivity.

Figure 15 shows three wind fields for 22:10 Greenwich mean time (GMT). A gust front and its associated reflectivity thin line can be seen to the east of the airport. This gust front was generated from a storm east of the coast. A convergence pocket in the wind field exists southwest of the airport. Just after this convergence pocket developed, a storm began to form at this location. The convergence strengthened along with the reflectivity associated with the growing storm. This coupling of convergence and storm

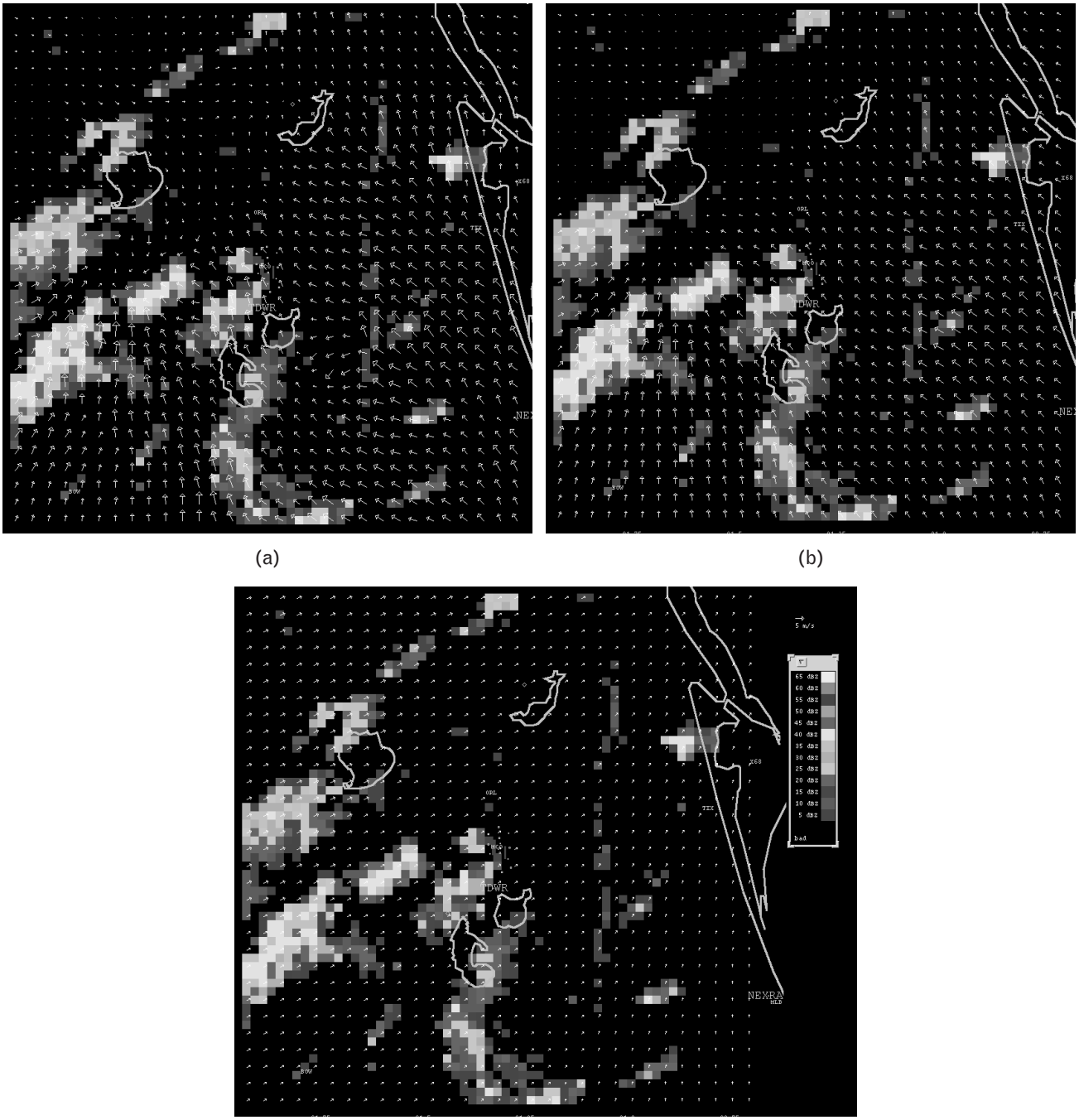

FIGURE 15. Wind-field analyses around Orlando on 20 August 1992 at 22:10 Greenwich mean time (GMT). (a) The 2-km-resolution optimal-estimation wind field, (b) the 10-km-resolution optimal-estimation wind field, and (c) the MAPS wind field. Each of these wind fields is displayed on the same 4-km-resolution grid for comparison. Orlando International Airport is at the center of each grid, and the east coast of Florida is shown at the right. The wind vectors are scaled to wind speed, with a 5-m/sec reference vector shown in the upper right corner of part *c*.

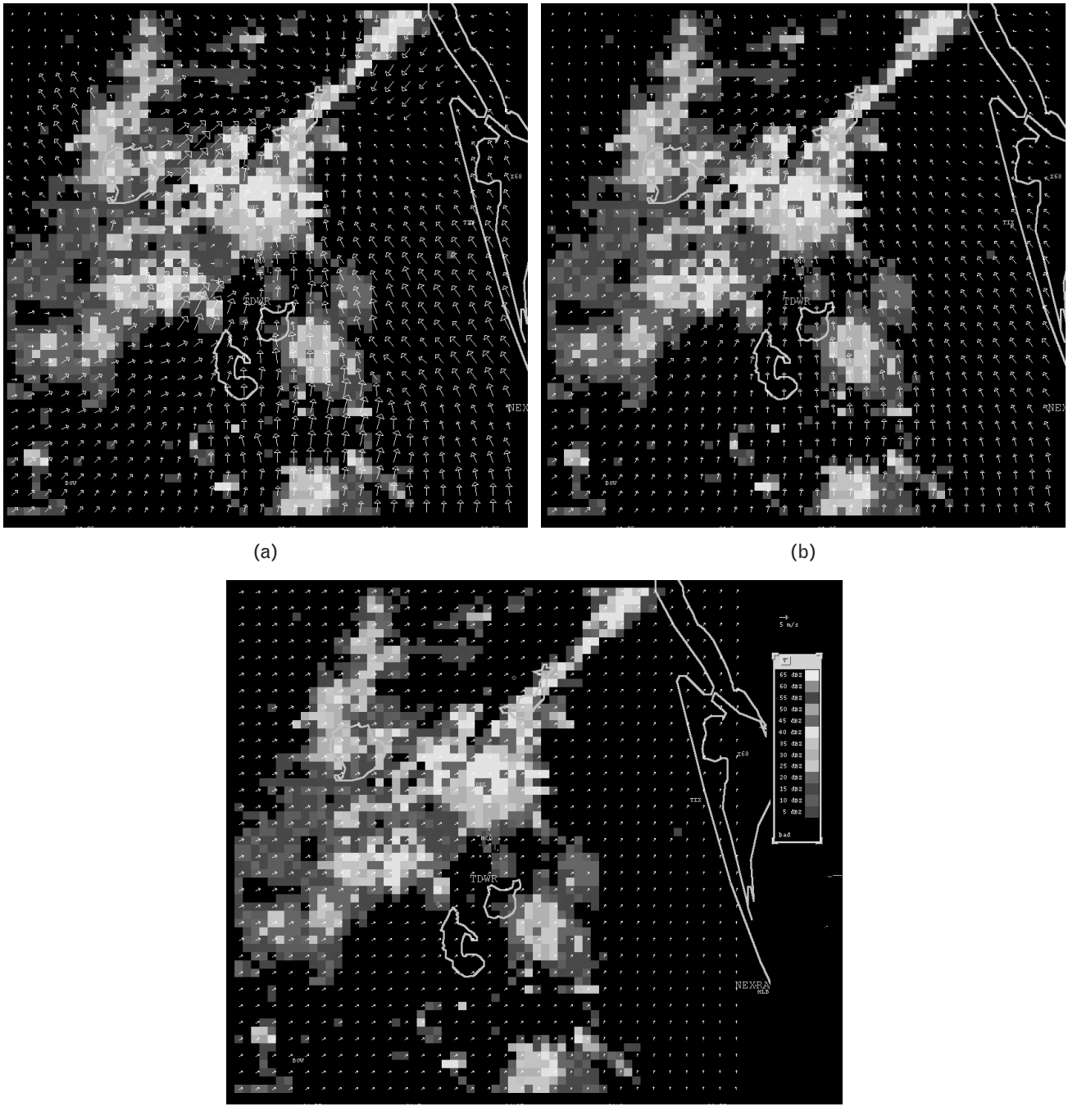

(a) (b)

(c)

FIGURE 16. Wind-field analyses around Orlando on 20 August 1992 at 23:10 GMT, one hour after the wind fields shown in Figure 15. (a) The 2-km-resolution optimal-estimation wind field, (b) the 10-km-resolution optimal-estimation wind field, and (c) the MAPS wind field. Each of these wind fields is displayed on the same 4-km-resolution grid for comparison. Orlando International Airport is at the center of each grid, and the east coast of Florida is shown at the right. The wind vectors are scaled to wind speed, with a 5-m/sec reference vector shown in the upper right corner of part *c*.

growth continued at various locations for the remainder of the afternoon. The lifting of water vapor in the atmosphere, and the resulting release of heat as the water vapor cools, is the driving force behind the formation of thunderstorms. Forecasting the formation of these storms requires that the wind-field convergence, and hence the vertical motion of the air, be correctly analyzed.

The 2-km-resolution Terminal Winds analysis shown in Figure 15(a) provides an excellent resolution of both the wind-field convergence associated with the gust front, and the convergence pocket southwest of the airport. The 10-km-resolution Terminal Winds analysis shown in Figure 15(b) captures these features, but underestimates the magnitude of the convergence and is missing the detail contained in the finer-resolution analysis. The MAPS forecast field shown in Figure 15(c) is not well correlated with the Terminal Winds analyses.

Figure 16 shows wind fields for 23:10 GMT, an hour later than the wind fields shown in Figure 15. The storm system generated by the convergence pocket seen at 22:10 GMT has grown into a large, strong convective storm that has evolved to the northeast of its original position. The 2-km-resolution Terminal Winds analysis shown in Figure 16(a) shows two regions of strong winds, northwest and southeast of the airport. The winds southeast of the airport began with the convergence pocket that existed at 22:10 GMT, and they started to die off after this time. The winds began to pick up in the region northwest of the airport at 22:40 GMT. These winds strengthened as the region of surface-wind convergence moved north along with the storm, and continued beyond the end of the day (24:00 GMT). The winds behind the gust front remained, although the gust-front thin line disappeared when the gust front collided with the storm system. The convection continued to build in the region of convergence that extends toward the northern boundary of the analysis. The 10-km-resolution Terminal Winds analysis shown in Figure 16(b) captures the general tendency of this convergence, but underestimates the strength of the stronger winds and the strength of the convergence. Again the MAPS forecast field shown in Figure 16(c) is not well correlated with the Terminal Winds–analyzed wind field.

Future Work

Two types of future work are discussed below. The first is analysis enhancements, including improvements to Terminal Winds and the development of a gridded temperature analysis. The second is real-time demonstrations at selected airports.

Analysis Enhancements

The ITWS gridded analysis system will undergo continued refinement and testing. A number of analysis upgrades are planned, including the use of the last analysis to refine the background wind field, the estimation and removal of errors arising from using an observation at locations away from the observation location, and the use of ITWS gust-front detections to increase the wind-field accuracy by suppressing averaging across the gust-front boundaries. A major effort will be undertaken to add surface forcing to refine the winds in the PBL, which is important for regions with coverage from only a single Doppler radar or with significant topographical variation. We are also assessing the ability of developing technologies to derive wind information from time variations in the radar reflectivity fields [15, 16]. When sufficiently developed, these technologies will be an important new source of wind information.

Accurate error models are required to ensure the success of any statistical technique. The volume of data at an ITWS site is not sufficient to estimate error models in real time; instead, we utilize *a priori* error models. Our current error models are qualitatively correct but can be refined on the basis of extensive examination of observed winds. A survey of the literature shows that past studies were conducted to construct error models for analyses with national or global domains in which observation separations are on the order of hundreds to thousands of kilometers. The results of these studies are not appropriate to error models for the Terminal Winds scale of analysis. We now have an archive of data including data from two summers and one winter in Orlando, and one summer in Memphis. We will use these data to construct quantitatively correct error models.

Starting in the summer of 1995, we will begin to develop a gridded temperature analysis. This analysis

will use a scalar version of the optimal-estimation winds analysis. The initial temperature-analysis system will use information from the RUC, MDCRS, and surface reports. The information from these sources will support a temperature analysis on the Terminal Winds 10-km-resolution grid. The temperature field and wind field are linked through physical processes. In an ITWS the wind field is known more precisely than the temperature field, so the knowledge of the wind field can be exploited to refine the temperature field. Current research at the University of Oklahoma and at NCAR provides techniques to retrieve temperature fields from wind fields. After development of the initial temperature analysis, we will assess the ability of the temperature retrieval to refine the temperature field.

Real-Time Demonstrations

A number of real-time demonstrations are planned. The ITWS had an FAA Demonstration and Evaluation at Memphis during the spring and summer of 1994, and at Orlando during the winter of 1995. The Demonstration and Evaluation continues at Dallas–Fort Worth in the summer of 1995 in conjunction with the Terminal Air Traffic Control Automation–Center TRACON Advisory System, which is the primary initial customer of the Terminal Winds information, and at Memphis. These Demonstration and Evaluation exercises will provide valuable testing in a variety of meteorological environments.

Summary

The Terminal Winds analysis is an important component of the ITWS. The Terminal Winds provides an accurate, high-resolution analysis of the horizontal winds in a three-dimensional grid in the terminal area. The wind information from this system is provided to a number of users, including air traffic automation systems and other ITWS algorithms. Terminal Winds combines wind information from a national-scale numerical-forecast model, meteorological Doppler radars, commercial aircraft, and anemometer networks. It is flexible enough to run reliably with any available subset of these data, adding value to the national winds forecast in the terminal area as local sensors provide information. The Terminal Winds system operated in the summers of 1992 and 1993 and the winter of 1995 in the Lincoln Laboratory ITWS testbed at Orlando, Florida, and in the spring and summer of 1994 at Memphis. The Terminal Winds system has demonstrated that it is a reliable operational system incorporating data from multiple sources, including operational TDWR and NEXRAD Doppler radars.

The terminal airspace extends from the surface to 18,000 feet above ground level, and is divided into two regimes. The planetary boundary layer (PBL) contains the atmosphere near the Earth's surface, and often contains wind structures with spatial scales on the order of kilometers and temporal scales on the order of minutes. Above the PBL, wind structures typically have spatial scales of at least tens of kilometers and temporal changes occur over at least tens of minutes. Doppler radars provide high-resolution information in the PBL, where small-scale wind structures are expected. Above the PBL, Doppler information becomes more sparse and the RUC and MDCRS are important sources of additional information. A cascade-of-scales analysis is used to capture these different scales of atmospheric activity.

A new winds-analysis technique, optimal estimation, was developed for the Terminal Winds product. This technique is an extension of both optimal interpolation and multiple-Doppler analysis. Under certain restrictive hypotheses, high-quality estimates of the horizontal winds can be derived from multiple-Doppler data sets. The ITWS will usually have data from at least two Doppler radars. Optimal interpolation, a statistical interpolation technique, is used in the current state-of-the-art operational non-Doppler winds analysis. Optimal estimation provides wind estimates that are of higher quality than multiple-Doppler analysis and does not suffer from the numerical instabilities that arise in multiple-Doppler analysis. The optimal-estimation analysis also produces wind vectors that vary smoothly between regions with coverage from differing numbers of Doppler radars.

The ITWS gridded analysis system will undergo continued refinement and testing. A number of analysis upgrades are planned, including the use of the last analysis to refine the background wind field, the estimation and removal of errors arising from estimat-

ing winds at locations removed from the observation location, and the use of ITWS gust-front detections to increase the wind-field accuracy. A major effort will be undertaken to add surface forcing to refine the winds in the PBL. We are also assessing the ability of developing technologies to derive wind information from radar reflectivity fields. When sufficiently developed, these technologies will be an important new source of wind information.

Acknowledgments

A number of people at NOAA/FSL provided important contributions to the Terminal Winds effort. In particular, we thank John McGinley and Steve Albers for the generous use of their Local Analysis and Prediction System code to build our initial prototype, and their many comments and general support. We also thank Thomas Schlatter and Stan Benjamin for providing wind forecasts from the Mesoscale Analysis and Prediction System. We thank the Melbourne National Weather Service Office for access to the NEXRAD base data. Providing this access was no mean feat. We also thank Russ Bolton and Jerry Starr at Computer Science–Raytheon for modifying their database to provide the off-airport ground-station data in our analysis region. Finally, we thank the LLWAS program office for expediting the installation of the LLWAS-3 anemometer network at the Orlando International Airport.

The development of the Terminal Winds system represents the combined efforts of a number of Lincoln Laboratory employees. Significant contributions were made by Steve Olson, Sue Yao, Cindy McLain, Russell Todd, Steve Kim, William Comery, Jim Cappucci, Gary Rasmussen, and Steve Finch.

REFERENCES

1. Seagull Technology, Inc., "Center-TRACON Automation System–Description to Support an Operational Concept Document," 90112-03 (1990).
2. F.W. Wilson, J. Keller, R.G. Rasmussen, and P. Zwack, "ITWS Ceiling and Visibility Products," *Fifth Int. Conf. on Aviation Weather Syst.*, *Vienna, VA, 2–6 Aug. 1993,* p. 51.
3. J.E. Evans and E.R. Ducot, "The Integrated Terminal Weather System (ITWS)," *Linc. Lab. J.,* in this issue.
4. R. Cole, F.W. Wilson, J.A. McGinley and S.C. Albers, "ITWS Gridded Analysis," *Fifth International Conference on Aviation Weather Syst., Vienna, VA, 2–6 Aug. 1993*, p. 56 (1993).
5. S.R. Finch, R.E. Cole, R.G. Rasmussen, F.W. Wilson, and S. Kim, "Summer 1992 Terminal Area—Local Analysis and Prediction System (T-LAPS) Evaluation," *ATC-218,* MIT Lincoln Laboratory (7 Oct. 1994), DOT/FAA/RD-94/13.
6. S.C. Albers, "The LAPS Wind Analysis," *Fourth Workshop on Operational Meteorology,* Whistler, BC, Canada (1992).
7. J. McGinley, S. Albers, and P. Stamus, "Validation of a Composite Convective Index as Defined by a Real-Time Local Analysis System," *Weather Forecast* **6,** 337 (1991).
8. M.W. Merritt, D. Klingle-Wilson, and S.D. Campbell, "Wind Shear Detection with Pencil-Beam Radars," *Linc. Lab. J.* **2,** 483 (1989).
9. T.D. Crum, R.L. Alberty, and D.W. Burgess, "Recording, Archiving, and Using WSR-88D Data," *Bull. Amer. Meteor. Soc.*. **74,** 645 (1993).
10. S.G. Benjamin, K.A. Brewster, R. Brümmer, B.F. Jewett, T.W. Schlatter, T.L. Smith, and P.A. Stamus, "An Isentropic Three-Hourly Data Assimilation System Using ACARS Aircraft Observations," *Mon. Weather Rev.* **119,** 888 (1991).
11. F.W. Wilson and R.H. Gramzow, "The Redesigned Low Level Wind Shear Alert System," *Fourth Int. Conf. on Aviation Weather Syst.*, *Paris*, *24–28 June 1991,* p. 370.
12. ASOS Program Office Staff, "Automated Surface Observing System Users Guide–Preliminary," National Weather Service ASOS Program Office, 84 pp. (1991). [Available from NWS ASOS Program Office, Silver Spring, MD 20910.]
13. K.A. Brewster, S.G. Benjamin, and R. Crawford, "Quality Control of ACARS Meteorological Observations—A Preliminary Data Survey," Preprints, *Third Int. Conf. on Aviation Weather Syst., Anaheim, CA, 30 Jan.–3 Feb. 1989,* p. 124.
14. L. Armijo, "A Theory for the Determination of Wind and Precipitation Velocities with Doppler Radars," *J. Atmospheric Sciences* **26**, 570 (1969)
15. C.-J. Qui and Q. Xu, "A Simple Adjoint Method of Wind Analysis for Single-Doppler Data," *J. Atmos. Oceanic Technol.* **9,** 588 (1992).
16. J.D. Tuttle and G.B. Foote, "Determination of the Boundary Layer Airflow from a Single Doppler Radar," *J. Atmos. Oceanic Technol.* **7**, 218 (1990).
17. D.G. Luenberger, *Optimization by Vector Space Methods* (Wiley, New York, 1969).
18. L.S. Gandin, "Objective Analysis of Meteorological Fields," Leningrad, translated by Israel Program for Scientific Translations, Jerusalem, 1965 (1963).
19. R. Daley, "Atmospheric Data Analysis" (Cambridge University Press, Cambridge, UK, 1991).
20. F.P. Bretherton and J.C. McWilliams, "Estimations from Irregular Grids," *Reviews of Geophysics and Space Physics* **18,** 789 (1980).
21. A.F. Bennett, "Inverse Methods in Physical Oceanography" (Cambridge University Press, Cambridge, UK, 1992).
22. M. Cairns et al., "A Preliminary Evaluation of Aviation-Impact Variables Derived From Numerical Models," NOAA Tech. Memo. ERL FSL-5 (1993).

RODNEY E. COLE
is a staff member in the Weather Sensing group. His research interests are in automated weather analysis and forecast algorithms, and linear and nonlinear optimization. He received a B.S. degree with a double major in mathematics and physics from the Virginia Polytechnic Institute and State University (VPI), an M.S. degree in mathematics from VPI, and a Ph.D. degree in mathematics from the University of Colorado at Boulder. Before joining Lincoln Laboratory in 1990, he worked at the National Center for Atmospheric Research. His first project as a staff member at Lincoln Laboratory was to lead the integration of the Terminal Doppler Weather Radar (TDWR) system and the Low Level Wind Shear Alert System (LLWAS) III, which is currently being installed in the field.

WESLEY F. WILSON
is a staff member in the Weather Sensing group. His primary focus of research is in the development of weather nowcast algorithms. He received B.S. and Ph.D. degrees in mathematics from the University of Maryland. He was an assistant professor of mathematics at Brown University in 1965 and the University of Michigan in 1966, and a professor of mathematics at the University of Colorado at Boulder from 1967 to 1987. Before joining Lincoln Laboratory in 1990 he worked at the National Center for Atmospheric Research. In 1992 Wes received the *Aviation Week* Lauriat Award for his invention of the Low Level Wind Shear Alert System (LLWAS) III, which was credited with saving a commercial aircraft from a wind-shear crash in Denver on 8 July 1989.